

# A Generalized Model to Predict the Viscosity of Solutions with Suspended Particles. III. Effects of Particle Interaction and Particle Size Distribution

RICHARD D. SUDDUTH

713 Mountain Gap Road, Huntsville, Alabama 35803

## SYNOPSIS

The generalized suspension viscosity equation utilized in this study was evaluated with both a packing fraction,  $\varphi_n$ , and a particle interaction coefficient,  $\sigma$ , as a function of suspension blend composition,  $f_{2T}$ . The estimation of the packing fraction,  $\varphi_n$ , in turn, required the further elucidation of the  $D_5/D_1$  ratio of particle diameter averages. Blend constants developed in this study allowed evaluation of both the  $D_x/D_y$  ratio of particle diameter averages as well as the number-average particle diameter,  $D_1$ , as a function of the fraction of one suspension in a blend,  $f_{2T}$ . These blend constants were shown to be easily evaluated from each individual suspension prior to blending. The viscosity data of Johnson and Kelsey were shown to be generally predicted as a function of the volume composition when a constant particle interaction coefficient,  $\sigma$ , was assumed. However, a better prediction of the results of Johnson and Kelsey was obtained by assuming that the particle interaction coefficient,  $\sigma$ , was a function of the number-average particle diameter,  $D_1$ , of the suspension mixture composition. Consequently, a new approach was identified to evaluate the simultaneous effects of small particles to both increase viscosity as a result of increasing particle interaction as well as to decrease viscosity as a result of improving the particle-size distribution. © 1993 John Wiley & Sons, Inc.

## INTRODUCTION

Over the years many equations have been developed to predict a relationship between suspension viscosity,  $\eta$ , and the volume fraction of suspended particle,  $\varphi$ . The applications and needs for such equations cross many disciplines. For example, the need to understand the viscosity of spherical particle suspensions was recognized early in the development of latexes to make synthetic rubber.<sup>1-4</sup> Paint and coatings latex development<sup>5,6</sup> has also found a need for this technology. Other diverse suspensions that have utilized this technology have included the food industry to evaluate milk<sup>7</sup> as well as the coal industry to evaluate bitumen emulsions.<sup>8</sup> More recently, this technology has also been applied to filled thermoplastics.<sup>9-11</sup> However, the new emerging thermoplastic particulate-filled thermoset resins of the type recently described by Recker et al.<sup>12</sup> would

probably be described as one of the types of materials currently most in need of a better understanding of the relationship between particle-size distribution and viscosity.

Several recent reviews<sup>11,13-16</sup> have addressed the current understanding of particle size and particle-size distribution on the rheology of suspensions. In a recent paper by this author,<sup>17</sup> a new generalized viscosity-concentration equation was described that combines many suspension viscosity-concentration equations summarized from the literature by Rutgers.<sup>18,19</sup> This new generalized equation, like most in the literature, utilizes a maximum particle packing fraction,  $\varphi_n$ , in the evaluation of suspension viscosity. Several attempts have been made in the literature<sup>20-22</sup> to predict the correct value for  $\varphi_n$  based on particle-size distribution. A new approach to evaluate  $\varphi_n$  for suspensions with binary particle combinations was recently introduced by this author.<sup>23</sup> This analysis process will be extended in this study to include techniques to evaluate  $\varphi_n$  for binary

combinations of suspensions, each of which may contain a wide distribution of particles.

### APPLICATION OF MAXIMUM PACKING FRACTION, $\varphi_n$ , TO A SPECIFIC GENERALIZED SUSPENSION VISCOSITY EQUATION

A generalized suspension viscosity equation that describes most of the primary equations identified by Rutgers<sup>18,19</sup> was recently introduced in the literature.<sup>17</sup> This viscosity-concentration equation that requires a value for the packing fraction,  $\varphi_n$ , is

$$\ln(\eta/\eta_0) = \left(\frac{[\eta]}{k}\right) \left(\frac{1}{\sigma-1}\right) \left\{ \frac{1 - (1 - k\varphi)^{\sigma-1}}{(1 - k\varphi)^{\sigma-1}} \right\}$$

for  $\sigma \neq 1$  (1)

For the case where  $\sigma = 1$ , the resulting equation can be written as

$$\eta = \eta_0 (1 - k\varphi)^{-[\eta]/k} \quad (2)$$

$$k = \frac{1}{\varphi_n} \quad (3)$$

where  $\eta$  is the suspension viscosity;  $\eta_0$ , the viscosity of suspending medium;  $[\eta]$ , the intrinsic viscosity;  $\sigma$ , the particle interaction coefficient;  $k$ , the "crowding factor";  $\varphi$ , the suspension particle volume fraction; and  $\varphi_n$ , the maximum particle packing fraction.

The intrinsic viscosity,  $[\eta]$ , is obtained at low concentration levels for the following limiting slope:

$$\text{as } \varphi \rightarrow 0, \text{ then } \frac{d \ln \eta}{d\varphi} \rightarrow [\eta] \text{ for all } \sigma \geq 0 \quad (4)$$

Some optional equations that can be developed using this generalized suspension viscosity equation are summarized in Table I along with authors<sup>1,4,24-27</sup> who first referenced some of these equations. As the particle interaction coefficient,  $\sigma$ , increases, the equations represented in Table I, have been shown to have a significantly faster rate of viscosity increase as a function of particle volume fraction. More importantly, the results in Table I show that fractional values of  $\sigma$  are also perfectly acceptable. Likewise, it should be noted that all of these equations with the exception of the case for  $\sigma = 0$  require the utilization of a maximum particle packing fraction,  $\varphi_n$ .

### GENERALIZED PARTICLE PACKING ANALYSIS FOR SUSPENSIONS WITH $n$ PARTICLE SIZES

A simplified technique was recently proposed<sup>17</sup> to estimate the packing fraction,  $\varphi_n$ , for any composition of particles in a suspension using the following equations:

$$\varphi_n = \varphi_{\text{mult}} - (\varphi_{\text{mult}} - \varphi_m) e^{\alpha[1 - (D_6/D_1)]} \quad (5)$$

**Table I** Generalized Suspension Viscosity Equation for Selected Values of the Particle Interaction Coefficient,  $\sigma$

Particle Interaction Coefficient, $\sigma$	Simplified Form of Generalized Equation	Previous Reference for Equation Derivation
0	$\ln(\eta/\eta_0) = [\eta]\varphi$	Arrhenius <sup>26,27</sup>
0.5	$\ln(\eta/\eta_0) = \left(\frac{2[\eta]}{k}\right) \left[1 - (1 - k\varphi)^{0.5}\right]$	
1	$\ln(\eta/\eta_0) = \left(\frac{[\eta]}{k}\right) \ln(1 - k\varphi)$	Krieger-Dougherty <sup>4</sup>
2	$\ln(\eta/\eta_0) = [\eta] \left\{ \frac{\varphi}{1 - k\varphi} \right\}$	Mooney <sup>1</sup>
3	$\ln(\eta/\eta_0) = \left(\frac{[\eta]}{2}\right) \left\{ \frac{2\varphi - k\varphi^2}{(1 - k\varphi)^2} \right\}$	
4	$\ln(\eta/\eta_0) = \left(\frac{[\eta]}{3}\right) \left\{ \frac{3\varphi - 2k\varphi^2 + k^2\varphi^3}{(1 - k\varphi)^3} \right\}$	

$$\varphi_{\text{mult}} = 1 - (1 - \varphi_m)^n \quad (6)$$

where  $\varphi_{\text{mult}}$  is the ultimate packing fraction;  $\varphi_m$ , the monodisperse packing fraction;  $\varphi_n$ , the suspension packing fraction;  $\alpha$ , a constant; and  $n$ , the number of different particle diameter classes in suspension, where the definition of the  $D_x$  particle diameter averages,  $D_x$ , can be described in the following general form:

$$D_x = \frac{\sum_{k=1}^n N_k \mathcal{D}_k^x}{\sum_{k=1}^n N_k \mathcal{D}_k^{x-1}} \quad (7)$$

where  $D_x$  is the average particle-size diameter;  $\mathcal{D}_k$ , the diameter of particle size  $k$ ;  $N_k$  the number of  $k$  particles; and  $x$ , the exponent on  $\mathcal{D}_k$  specifying the particle-size diameter average.

Utilizing this calculation procedure, the value of  $\varphi_n$  can be evaluated for any ratio  $D_5/D_1$ . Evaluation of the  $D_5$  and  $D_1$  averages requires knowledge of the numbers of particles,  $N_i$ , and their diameters,  $\mathcal{D}_i$ , or another measure of the composition of the  $n$  different particle sizes in a suspension.

The ultimate packing fraction,  $\varphi_{\text{mult}}$ , obtained using the monodisperse limit for loose random packing or  $\varphi_m = 0.589$  has been shown<sup>17</sup> to normally be preferred when the number of  $n$  distinctly different particle sizes in a suspension is greater than  $n = 2$ . In addition, the specific  $D_5/D_1$  ratio particle diameter average was found to be the one that best predicted the packing fraction for binary particle compositions. Finally, it was suggested that the applicability of the  $D_5/D_1$  ratio should also be adequate to predict the packing fraction of binary combinations of two suspensions each with a broad distribution of particle sizes. This speculation will be addressed in this paper.

#### DERIVATION OF THE OPTIMUM BLEND FRACTION, $f_{2T}$ OF TWO SUSPENSIONS A AND B TO ACHIEVE A MAXIMUM RATIO OF PARTICLE-SIZE AVERAGES $D_x/D_y$ FOR THE COMBINED BLEND

To better understand the role the  $D_5/D_1$  ratio of particle-size averages plays in the determination of the suspension packing fraction,  $\varphi_n$ , it is useful to consider the  $D_x/D_y$  ratio of average particle sizes in general. The definition of the  $D_x$  particle diameter averages,  $D_x$ , can be described as indicated in eq. (7). For a blend of two suspensions, the  $D_x$  particle diameter averages can be rewritten as

$$D_x = \frac{\sum_{i=1}^n N_{1i} \mathcal{D}_{1i}^x + \sum_{j=1}^m N_{2j} \mathcal{D}_{2j}^x}{\sum_{i=1}^n N_{1i} \mathcal{D}_{1i}^{x-1} + \sum_{j=1}^m N_{2j} \mathcal{D}_{2j}^{x-1}} \quad (8)$$

where  $D_x$  is the average particle-size diameter;  $\mathcal{D}_{1i}$ , the diameter of particle size  $i$  in the first suspension;  $\mathcal{D}_{2j}$ , the diameter of particle size  $j$  in the second suspension;  $N_{1i}$ , the number of  $i$  particles in the first suspension; and  $N_{2j}$ , the number of  $j$  particles in the second suspension.

For a mixture of two suspensions, then, the ratio of a  $D_x$  average diameter to the  $D_y$  average diameter could be written as

$$\frac{D_x}{D_y} = \left\{ \frac{\sum_{i=1}^n N_{1i} \mathcal{D}_{1i}^x + \sum_{j=1}^m N_{2j} \mathcal{D}_{2j}^x}{\sum_{i=1}^n N_{1i} \mathcal{D}_{1i}^{x-1} + \sum_{j=1}^m N_{2j} \mathcal{D}_{2j}^{x-1}} \right\} \times \left\{ \frac{\sum_{i=1}^n N_{1i} \mathcal{D}_{1i}^{y-1} + \sum_{j=1}^m N_{2j} \mathcal{D}_{2j}^{y-1}}{\sum_{i=1}^n N_{1i} \mathcal{D}_{1i}^y + \sum_{j=1}^m N_{2j} \mathcal{D}_{2j}^y} \right\} \quad (9)$$

The process of simplifying eq. (9) begins by considering the volume fraction of different particles prior to blending. After two suspensions are blended, then the volume fraction of the first particle in the blend would be defined as

$$f_{11} = \frac{N_{11} \mathcal{D}_{11}^3}{\sum_{i=1}^n N_{1i} \mathcal{D}_{1i}^3 + \sum_{j=1}^m N_{2j} \mathcal{D}_{2j}^3} \quad (10)$$

Using volume fractions as described by eq. (10), the sum of all particle fractions in the blend would equal 1 as

$$f_{11} + f_{12} + f_{13} + \cdots + f_{1n} + f_{21} + f_{22} + f_{23} + \cdots + f_{2m} = 1 \quad (11)$$

or

$$f_{1T} + f_{2T} = 1 \quad (12)$$

where

$$f_{1T} = \sum_{i=1}^n f_{1i} \quad (13)$$

$$f_{2T} = \sum_{j=1}^m f_{2j} \quad (14)$$

At this point, starting from eqs. (10)–(14), the  $D_x/D_y$  ratio for the blending of two latexes described by eq. (9), can be simplified with the blend constants,  $a_1, a_2, b_1, b_2, c_1, c_2, d_1,$  and  $d_2$  derived and summarized in Appendix A to give

$$\frac{D_x}{D_y} = \left\{ \frac{a_1 + f_{2T}(a_2 - a_1)}{c_1 + f_{2T}(c_2 - c_1)} \right\} \left\{ \frac{b_1 + f_{2T}(b_2 - b_1)}{d_1 + f_{2T}(d_2 - d_1)} \right\} \quad (15)$$

The  $D_x/D_y$  ratio as defined by eq. (15) can be further simplified to give

$$\frac{D_x}{D_y} = \frac{A_1 f_{2T}^2 + B_1 f_{2T} + C_1}{A_2 f_{2T}^2 + B_2 f_{2T} + C_2} \quad (16)$$

where

$$A_1 = (a_2 - a_1)(b_2 - b_1)$$

$$B_1 = a_1(b_2 - b_1) + b_1(a_2 - a_1)$$

$$C_1 = a_1 b_1$$

$$A_2 = (c_2 - c_1)(d_2 - d_1)$$

$$B_2 = c_1(d_2 - d_1) + d_1(c_2 - c_1)$$

$$C_2 = c_1 d_1 \quad (17)$$

Note at this point that the ratio  $D_x/D_y$  can be obtained for any volume fraction of the second suspension,  $f_{2T}$ . The maximum value of  $D_x/D_y$  can be obtained from a plot of  $D_x/D_y$  vs.  $f_{2T}$ . It is also apparent, however, that the maximum can easily be calculated. The extrema for  $D_x/D_y$  can be obtained by taking the derivative of eq. (16) and setting it equal to zero as

$$\frac{d\left(\frac{D_x}{D_y}\right)}{df_{2T}} = 0 \quad (18)$$

The two roots of this equation are

$$f_{2T} = \frac{A_2 C_1 - A_1 C_2 + \sqrt{(A_2 C_1 - A_1 C_2)^2 - (C_2 B_1 - C_1 B_2)(A_1 B_2 - A_2 B_1)}}{A_1 B_2 - A_2 B_1} \quad (19)$$

and

$$f_{2T} = \frac{A_2 C_1 - A_1 C_2 - \sqrt{(A_2 C_1 - A_1 C_2)^2 - (C_2 B_1 - C_1 B_2)(A_1 B_2 - A_2 B_1)}}{A_1 B_2 - A_2 B_1} \quad (20)$$

Normally, only one of these roots gives values of  $f_{2T}$  between 0 and 1. When this root is substituted into eq. (16), the maximum value of  $D_x/D_y$  is obtained. A simple result is obtained for  $f_{2T}$  if each blended suspension is made up of only one particle size. The result for this case is

$$f_{2T} = \frac{1}{1 + \sqrt{R_{21/11}^{x+y-7}}} \quad (21)$$

where  $R_{21/11}$  is defined in Appendix A as

$$R_{21/11} = \frac{\mathcal{D}_{21}}{\mathcal{D}_{11}} \quad (22)$$

where  $\mathcal{D}_{11}$  and  $\mathcal{D}_{21}$  are diameters of the first or primary particles in each of the suspensions being blended.

This result for binary combinations of particles sizes was also obtained in an earlier paper by this author.<sup>23</sup> For binary particle blends, it is apparent from eq. (21) that the volume fraction where the  $D_x/D_y$  ratio is a maxima for ( $x = 5, y = 1$ ) is also

obtained when ( $x = 4, y = 2$ ). Further details of this relationship were discussed in some detail previously by this author<sup>23</sup> and will not be repeated here.

However, if the optimum volume fraction from eq. (21) is substituted into eq. (16), then the maximum value of  $D_x/D_y$  for binary combinations of particle sizes can be obtained as

$$\left(\frac{D_x}{D_y}\right)_{\max} = R_{21/11} \left\{ \frac{2R_{21/11}^{(y-x-1)/2} + R_{21/11}^{y-x-1} + 1}{2R_{21/11}^{(y-x+1)/2} + R_{21/11}^{y-x+1} + 1} \right\} \quad (23)$$

This result also agrees nicely with previously published results by this author.<sup>23</sup> It is apparent from eq. (23) that for binary combinations of particle sizes the same maximum value of  $D_x/D_y$  is obtained only when the difference between  $x$  and  $y$  is identical. An example of one of these groups of  $x$  and  $y$  that define identical maxima for all values of  $R_{21/11}$  would include

$$\left(\frac{D_3}{D_1}\right)_{\max} = \left(\frac{D_4}{D_2}\right)_{\max} = \left(\frac{D_5}{D_3}\right)_{\max} = \left(\frac{D_6}{D_4}\right)_{\max} \quad (24)$$

The significance of this point is that combinations of  $x$  and  $y$  that have the same location of the  $D_x/D_y$  maxima will not necessarily have the same value for  $(D_x/D_y)_{\max}$ .

Finally, it is interesting to note that when  $R_{21/11} = 1$  in eq. (21) that

$$f_{2T} = 0.5 \text{ for all values of } x \geq 1 \text{ and } y \geq 1 \quad (25)$$

This result is intuitively satisfying since it predicts that the maximum ratio for  $D_x/D_y$  would occur at a condition of equal volume when both particles are the same size.

### CALCULATION PROCEDURES UTILIZED TO ANALYZE THEORETICAL EQUATIONS

The characteristic  $D_x$  average particle diameters of either the individual suspensions or their blends calculated from the theoretical equations developed in this study require the following information:

- Profiles of particle diameters in each suspension or latex,  $D_{1i}$  or  $D_{2j}$ , as well as the numbers of these particles,  $N_{1i}$  or  $N_{2j}$ .

With this information, three approaches that can be used to analyze the formulation developed include

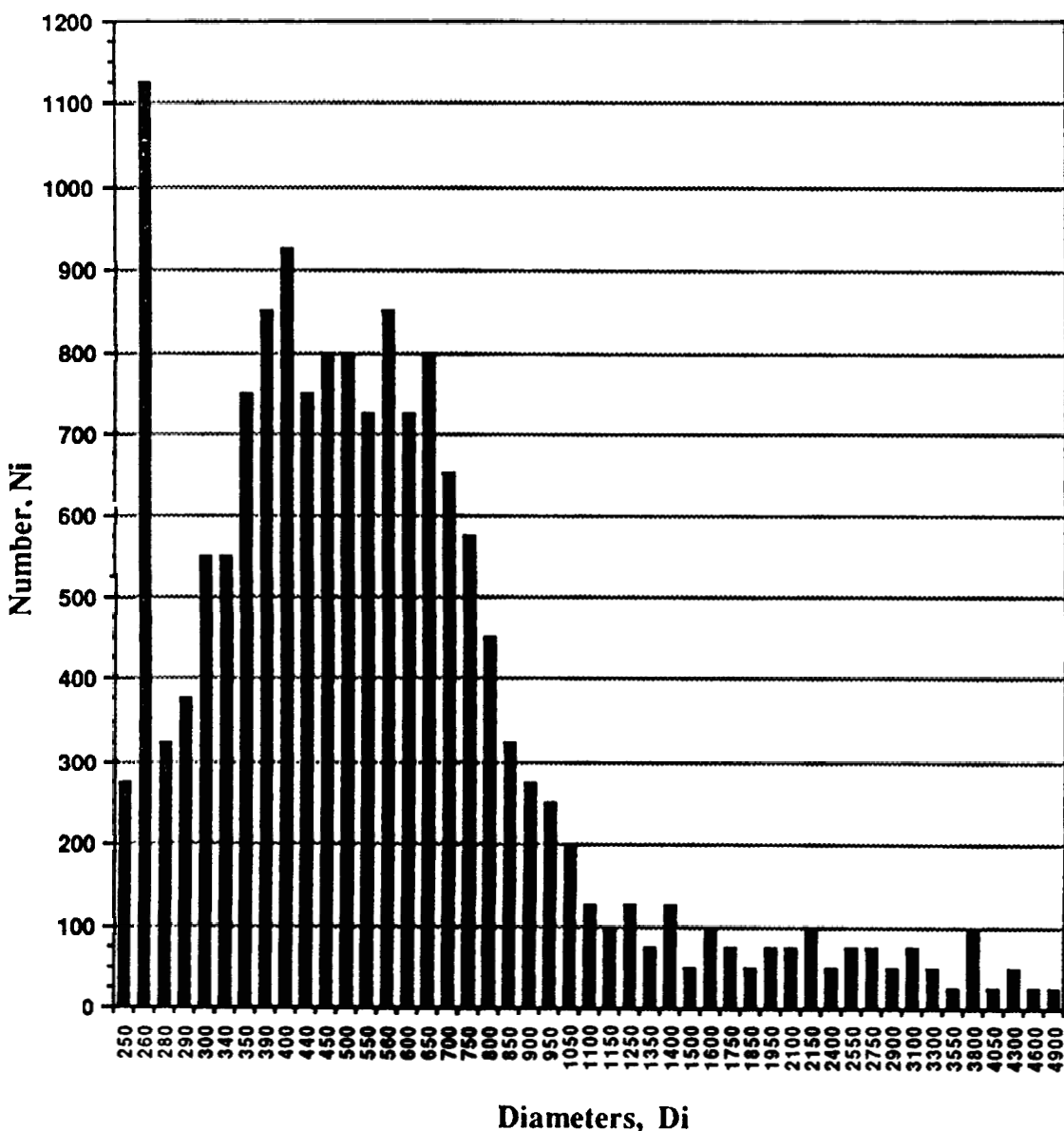
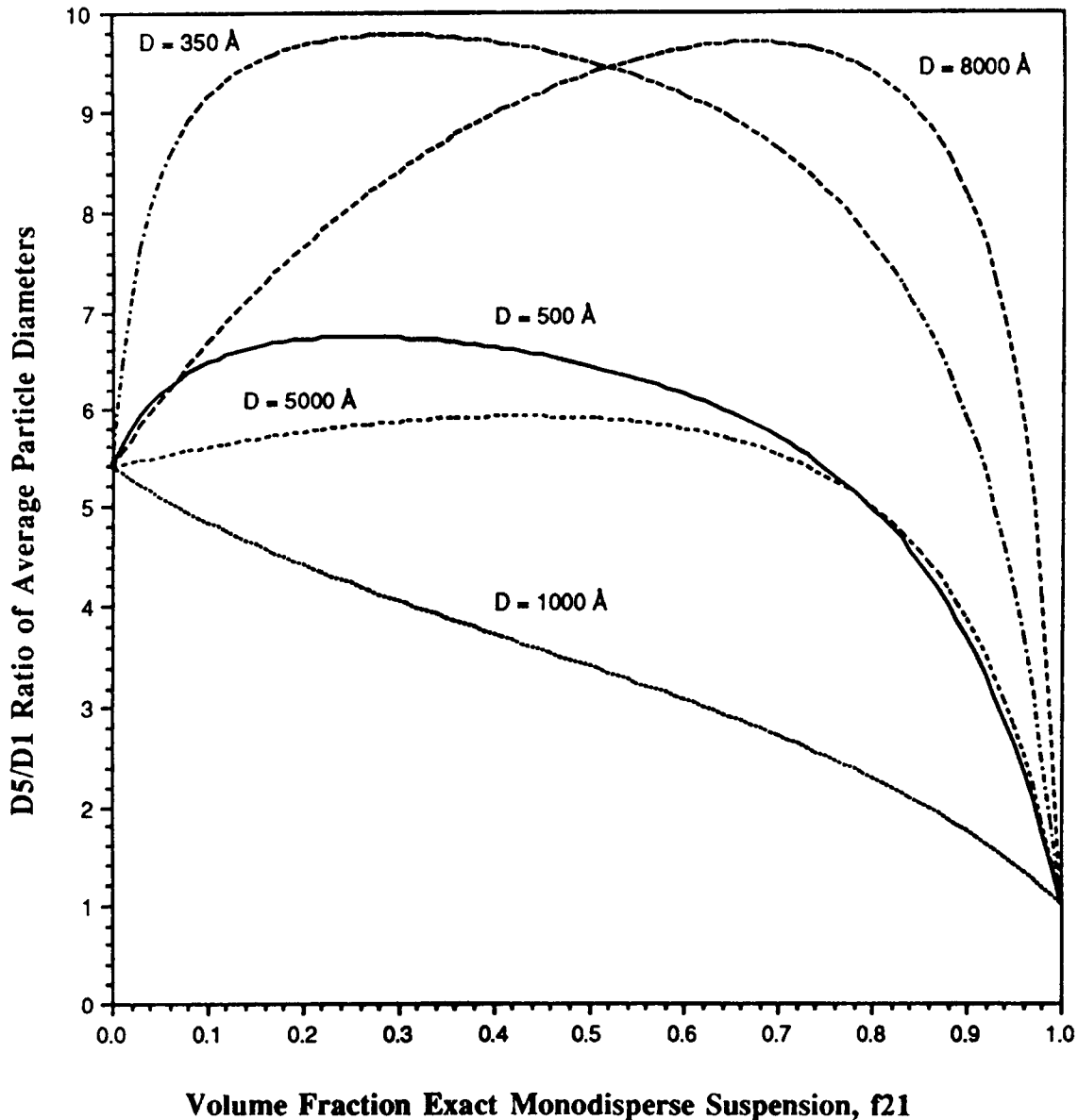


Figure 1 Example latex A particle diameter distribution.





**Figure 3** Calculated blends of a broad particle-size suspension, latex A, with exact monodisperse suspensions.

or (20). Again, the calculations of the constants  $A_1$ ,  $B_1$ ,  $C_1$ ,  $A_2$ ,  $B_2$ , and  $C_2$  in eq. (19) or (20) require additional calculations from eqs. (17) in the text and eqs. (A.8)–(A.12) and (A.22)–(A.29) in Appendix A.

Utilization of the three calculation procedures described above can provide a system of checks and balances to validate or verify the computer outputs for these results. All three techniques were used to validate the calculations presented in this study.

**BLENDING CALCULATIONS INVOLVING LATEX A CONSISTING OF A BROAD DISTRIBUTION PARTICLE DIAMETERS AND A MONODISPERSE LATEX CONSISTING OF ONLY ONE PARTICLE DIAMETER**

To illustrate the capability of the blending methodology introduced in this article, consider the example latex A described in Figure 1. This example latex has a broad distribution of particle sizes that can probably be best described in terms of a plot of

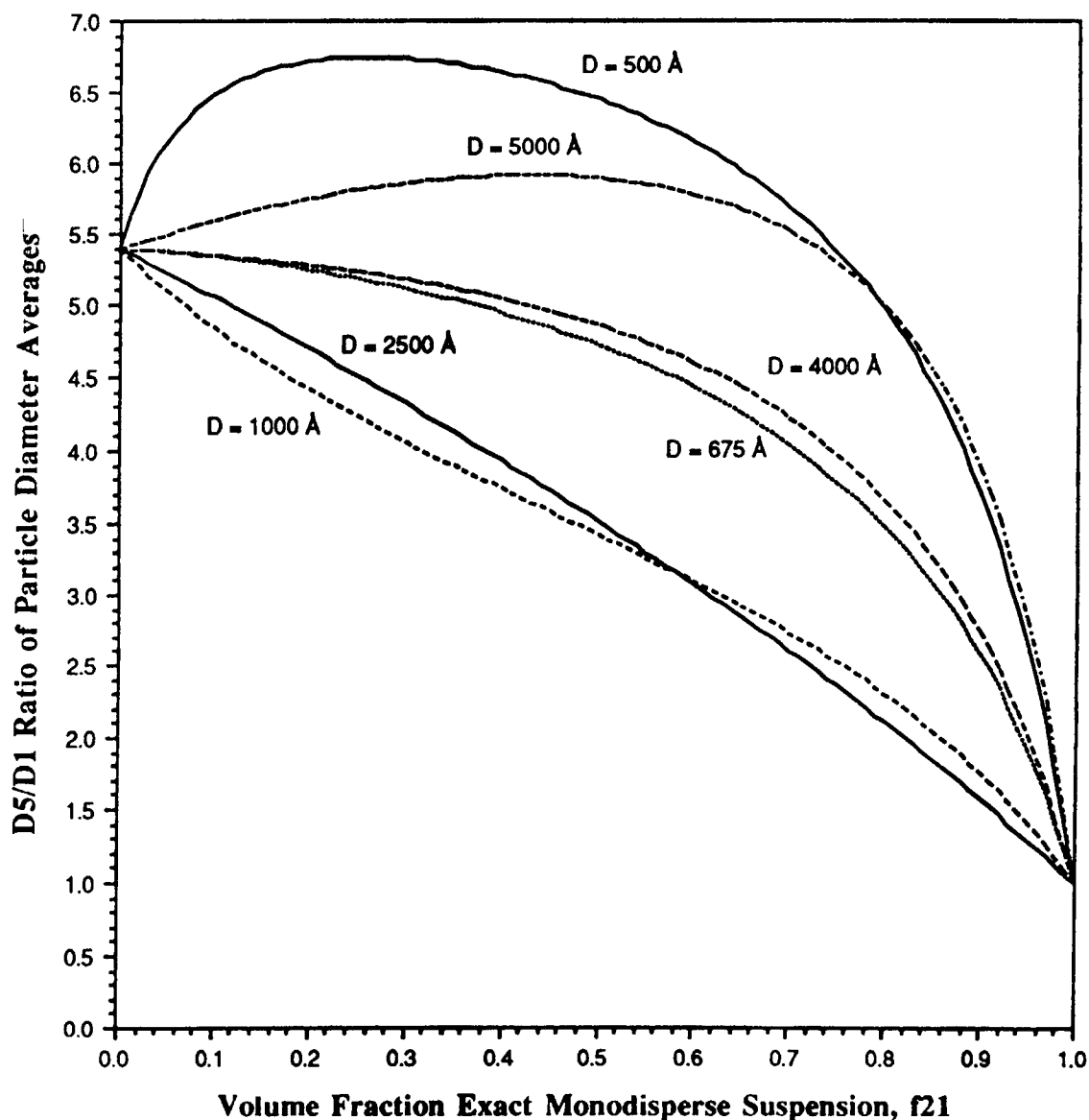


**Figure 4** Calculated blends of a broad particle-size suspension, latex A, with exact monodisperse suspensions.

its average particle diameters,  $D_x$ , described by eq. (7) as discussed earlier in this article. These  $D_x$  averages have been characterized by Herdan<sup>28</sup> who showed that

$$D_1 \leq D_2 \leq D_3 \leq \dots \leq D_n \quad (26)$$

A plot of the  $D_x$  averages vs.  $x$  for latex A are summarized in Figure 2. The question then arises as to which average particle diameter best characterizes this latex. The number-average particle diameter,  $D_1$ , tends to weight the small particle sizes more than it does the large diameter particles. However,

the actual volume of small particles is often much less than the large particle diameters. On the other hand, the  $D_8$  average particle diameter tends to weight the large particle diameters more than it does the small ones.

In an earlier article by this author,<sup>29</sup> it was shown theoretically that the surface average particle diameter,  $D_3$ , was the correct average to use to predict impact in two-phase plastics. The surface average tends to weigh both the small particle sizes and the large particle sizes nearly equally to give a good characteristic average particle diameter of a mixture of particles. For this reason, the surface average,  $D_3$ ,



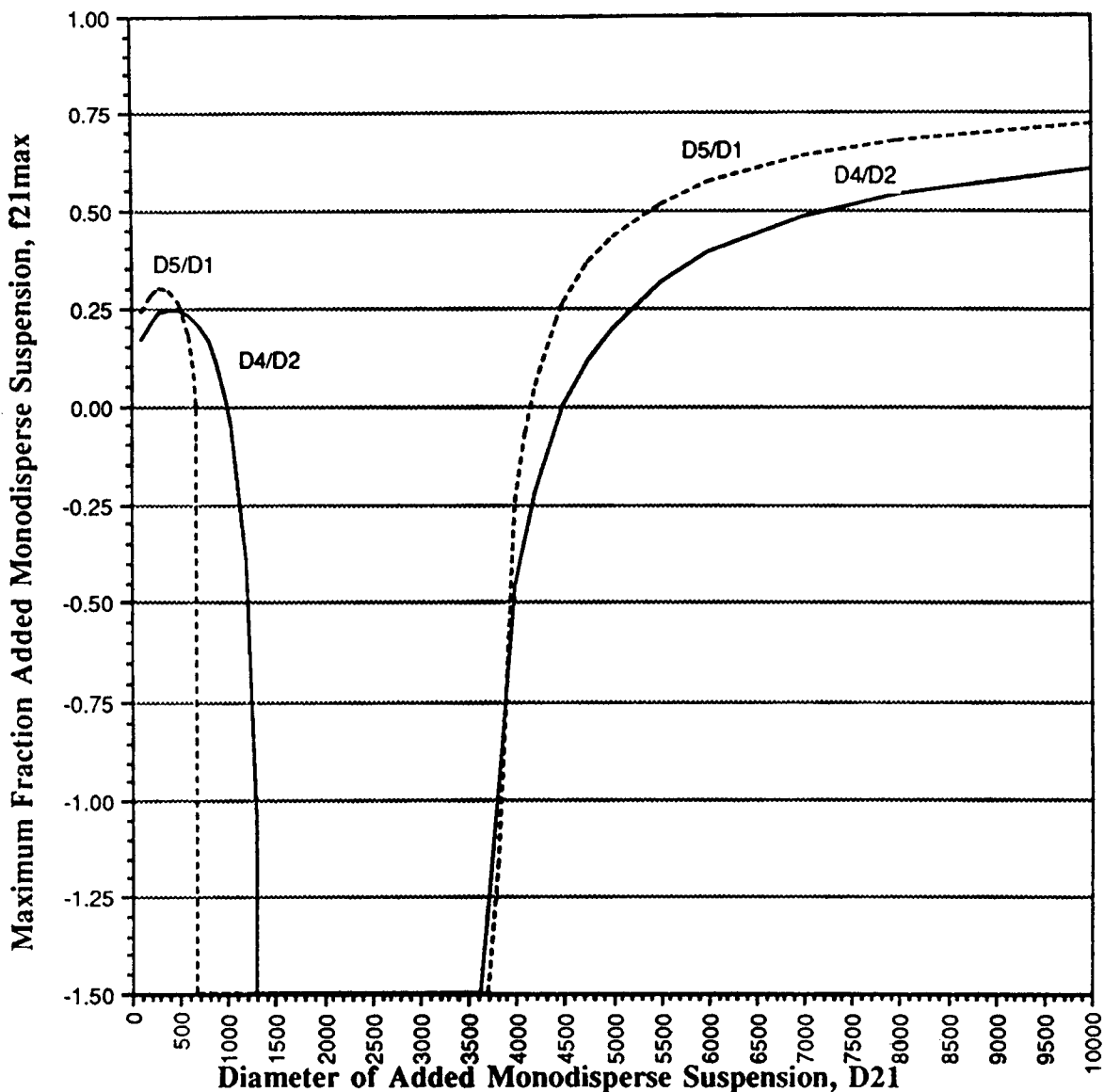


Figure 5 Calculated fraction of added monodisperse suspension at the maximum  $D_5/D_1$  or  $D_4/D_2$  average particle-size ratios.

usually is often used to characterize the average particle diameter in a suspension.

Theoretical blend spectrums of particle-size distributions as measured by the  $D_5/D_1$  particle average ratio for latex A with several different monodisperse latexes are shown in Figure 3 (assuming diameters of latex A measured in Å). The monodisperse latexes blended with latex A to generate Figure 3 contained only one particle diameter size. With the monodisperse latexes defined in this way, the following volume fractions are equivalent:

$$f_{2T} = f_{21} \quad (27)$$

Note that not all absolute monodisperse particles latexes can improve latex A. The maximum ratio of  $D_5/D_1$  for the 1000 Å monodisperse latex occurs for the pure latex A. Any amount of the 1000 Å latex added to latex A only tends to decrease the  $D_5/D_1$  ratio. The range of monodisperse particle latexes that do not improve latex A are illustrated in Figure 4.

The monodisperse latex volume fractions,  $f_{21}$  or  $f_{2T}$ , that locate the maximum  $D_5/D_1$  ratios illustrated in Figures 3 and 4 have been calculated using either eq. (19) or (20) and are summarized in Figure 5. The results in Figure 5 illustrate the location of

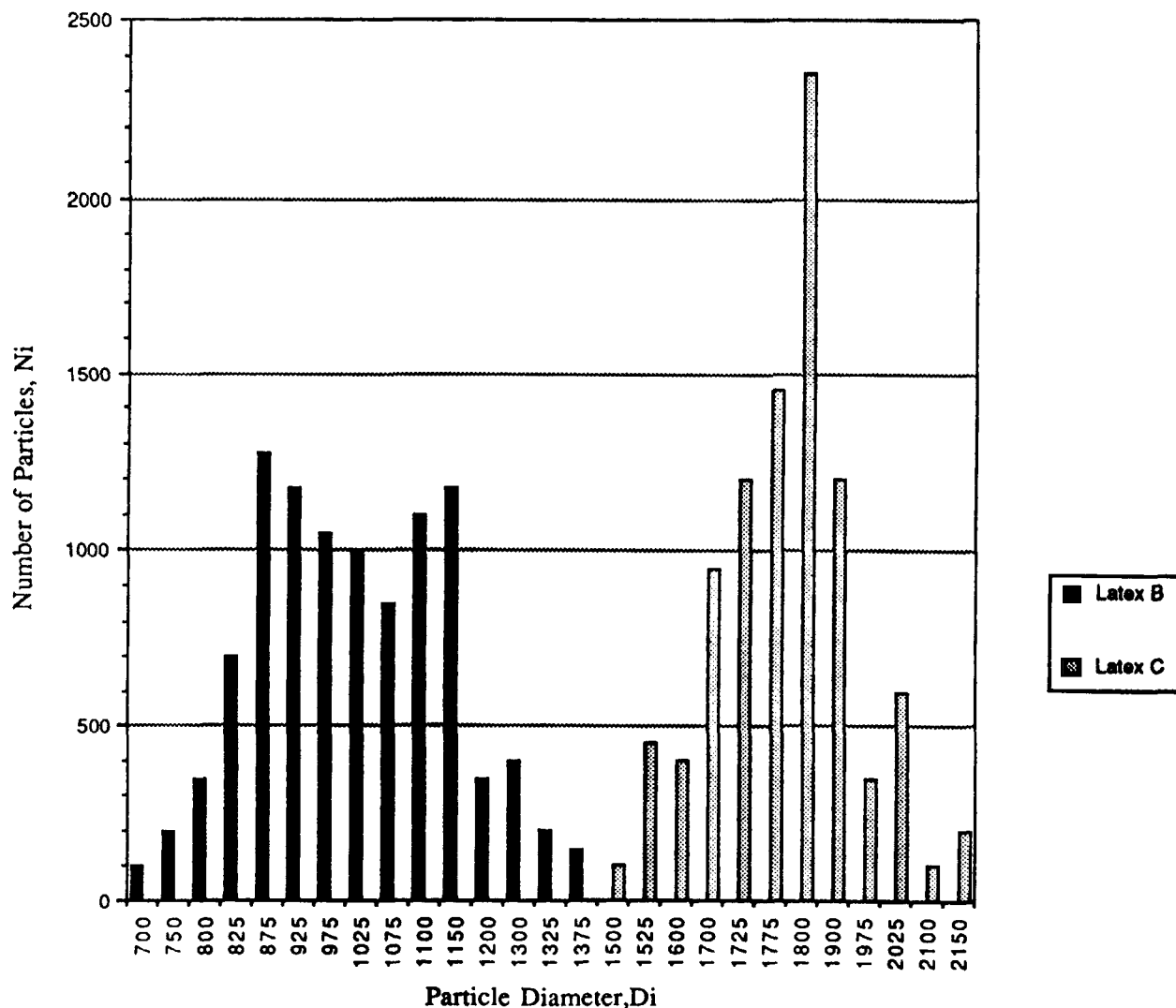


Figure 6 Particle distributions for latexes B and C.

the optimum blends of latex A with the appropriate monodisperse latex. Also included in Figure 5 are the optimum blends with latex A for the  $D_4/D_2$  ratio. As shown theoretically, earlier, both the  $D_5/D_1$  and the  $D_4/D_2$  ratios gave the same location for blends of two exactly monodisperse latexes. However, when a broad particle-size suspension like latex A is blended with an exactly monodisperse latex, it is apparent that the  $D_5/D_1$  and the  $D_4/D_2$  ratios do not give the same location of the optimum blends. The significance of the negative optimum values of  $f_{21}$  in Figure 5 means that the maximum value of the  $D_5/D_1$  or the  $D_4/D_2$  occurs for the original latex A. Any amount of monodisperse latex for these cases reduces the ratio of particle-size averages. Single-particle-size monodisperse latexes that are not ef-

fective in improving either the  $D_5/D_1$  or the  $D_4/D_2$  distribution ratios for latex A include

Particle range for latex A giving negative  $f_{21}$  for

$$(D_5/D_1)_{\max} = 673-4158 \text{ \AA} \quad (28)$$

Particle range for latex A giving negative  $f_{21}$  for

$$(D_4/D_2)_{\max} = 1009-4506 \text{ \AA} \quad (29)$$

#### BLENDING CALCULATIONS INVOLVING TWO LATEXES EACH CONTAINING A DISTRIBUTION OF PARTICLE DIAMETERS

To further illustrate the capability of the blending methodology introduced in this paper, consider the

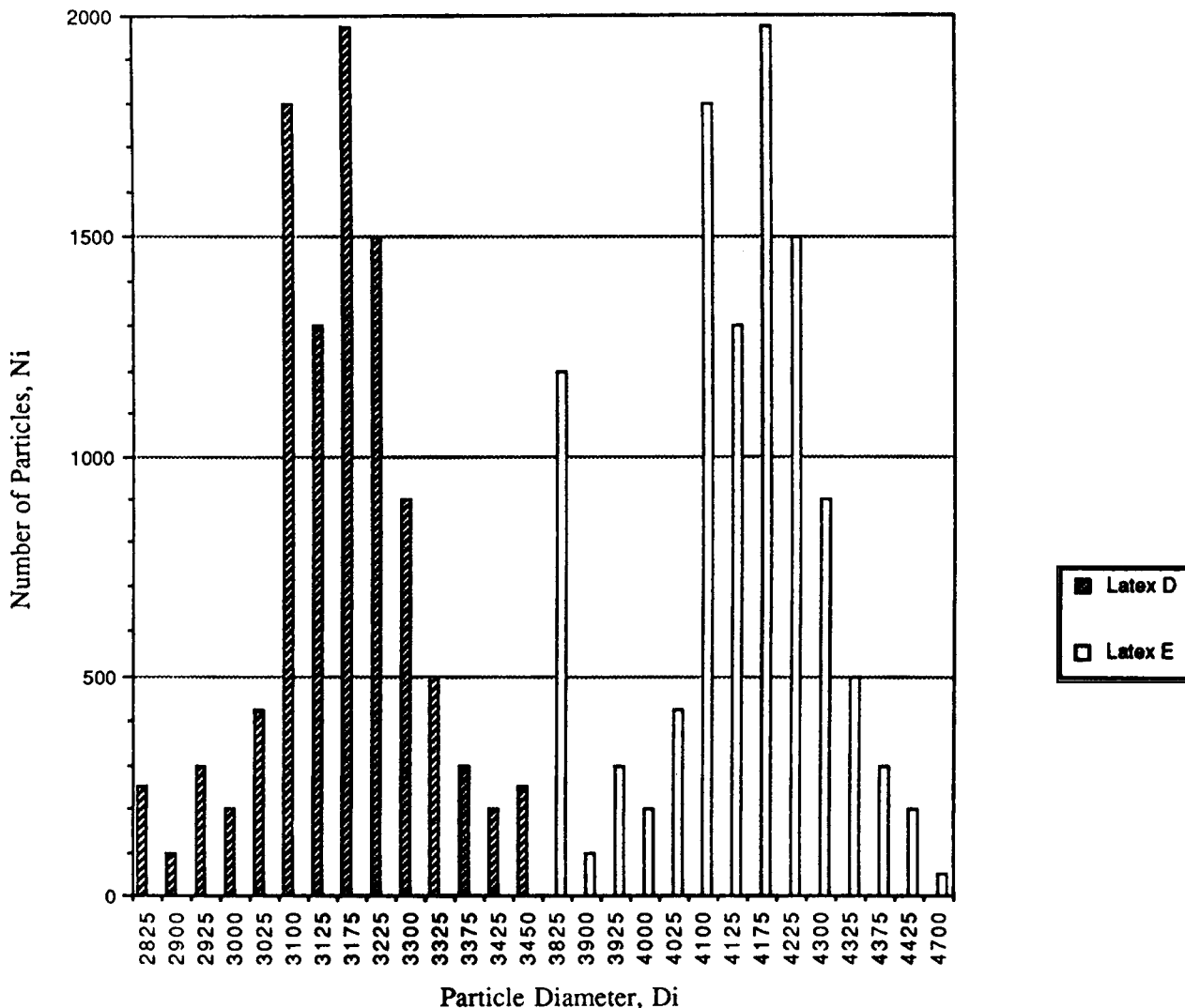


Figure 7 Particle distributions of latexes D and E.

four latex distributions illustrated in Figures 6 and 7. The  $D_x$  averages for latexes B, C, and D are summarized in Table II. The distribution for the three latexes B, C, and D were extracted from an article by Johnson and Kelsey.<sup>3</sup> These latexes each have multiple particles but are reasonably monodisperse. For comparison, the full range of blends of latex B with D have been included in Figure 8 for different  $D_x/D_1$  ratios as a function of the volume fraction of latex D. It is apparent in this figure that the maximum value for  $D_x/D_1$  increases with the value of  $x$ . However, the location of the maximum is obviously different for each value of  $x$ . As discussed earlier for a blend of latexes each consisting of only one particle size, combinations of  $D_x/D_y$  with the same value of  $x + y - 7$  should have the same location for  $(D_x/$

$D_y)_{\max}$ . For example, from eq. (21), it would be anticipated that ratios  $D_5/D_1$  and  $D_4/D_2$  should have nearly the same location of the maximum values for these ratios when blending near monodisperse latexes like B and D. The full range of blends for these ratios is included in Figure 9. As expected, the location of these maxima are indeed nearly identical. In particular, these values are

$$f_{2T} = 0.633 [\text{for } (D_5/D_1)_{\max}] \quad (30)$$

and

$$f_{2T} = 0.628 [\text{for } (D_4/D_2)_{\max}] \quad (31)$$

Although these values are not identical, they are extremely close. For comparison, the equivalent

**Table II**  $D_x$  Particle Diameter Averages for Latexes B, C, and D (LB, LC, and LD)

$X$	$D_x$ (LB)	$D_x$ (LC)	$D_x$ (LD)	$D_x$ (LC)/ $D_x$ (LB)	$D_x$ (LD)/ $D_x$ (LC)	$D_x$ (LD)/ $D_x$ (LB)
1	1013.90	1795.86	3170.25	1.771	1.765	3.127
2	1035.16	1805.54	3175.24	1.744	1.759	3.067
3	1056.44	1815.33	3180.17	1.718	1.752	3.010
4	1077.50	1825.26	3185.05	1.694	1.745	2.956
5	1098.14	1835.33	3189.89	1.671	1.738	2.905
6	1118.17	1845.56	3194.68	1.651	1.731	2.857
7	1137.44	1855.95	3199.43	1.632	1.724	2.813
8	1155.84	1866.49	3204.14	1.615	1.717	2.772
$f_{2T}$ with latex A ( $D_5/D_1$ )	Imaginary	Imaginary	Imaginary			
$f_{2T}$ with latex A ( $D_4/D_2$ )	-0.0340115	Imaginary	Imaginary			
Monodisperse diameter negative blend range with latex A ( $D_5/D_1$ )	673-4158					
Monodisperse diameter negative blend range with latex A ( $D_4/D_2$ )	1009-4506					

$R_{21/11}$  ratio of absolute monodisperse latexes for the  $f_{2T}$  values above can be calculated using eq. (21) to give

$$R_{21/11} = 2.965 \text{ [ for } (D_5/D_1)_{\max} \text{ ]} \quad (32)$$

and

$$R_{21/11} = 2.860 \text{ [ for } (D_4/D_2)_{\max} \text{ ]} \quad (33)$$

As indicated in Table II, the ratio of  $D_x$  for latexes D and B that comes closest to these  $R_{21/11}$  ratios would be  $D_4$  for  $D_5/D_1$  and  $D_6$  for  $D_4/D_2$ . However, the  $D_3$  ratio satisfactorily predicts the upper limit of  $R_{21/11}$  that could reasonably be expected for either  $D_5/D_1$  or  $D_4/D_2$ .

In addition, eq. (23) for exactly monodisperse latexes predicts that

$$\begin{aligned} \left(\frac{D_3}{D_1}\right)_{\max} &= \left(\frac{D_4}{D_2}\right)_{\max} = \left(\frac{D_5}{D_3}\right)_{\max} = \left(\frac{D_6}{D_4}\right)_{\max} \\ &= \left(\frac{D_7}{D_5}\right)_{\max} = \left(\frac{D_8}{D_6}\right)_{\max} \end{aligned} \quad (34)$$

A comparison of these ratios has been included in Figure 10 for the range of blends for latexes B and D. Again, it is apparent that these maxima do not all have exactly the same value. However, when

compared to the range of maxima in Figure 8, they do indeed have maxima that are approximately the same order of magnitude.

Note that all  $D_x$  averages for latexes B, C, and D blended with latex A fall within the range that would be expected to give a negative  $f_{2T}$  for  $(D_5/D_1)_{\max}$  or  $(D_4/D_2)_{\max}$  ratios as indicated in eqs. (28) and (29). Calculations indeed show these expectations to be correct, as indicated in Table II. Blends of these latexes with latex A gave values of  $f_{2T}$  that are either negative or imaginary. For this reason, latex E as shown in Figure 7 was devised to explore the upper limits expected for the negative  $f_{2T}$  range for blends with latex A. The results of these calculated blends of latex E and modifications of latex E with latex A are summarized in Table III. The modifications to latex E were made by changing the number of particles of the smallest particle size,  $N_{21}$ , or the number of the largest particles,  $N_{2n}$ , in latex E.

The results in Table III indicate clearly that the  $D_5$  average appears to control the upper limit of  $f_{2T}$  for the  $D_5/D_1$  ratio and the  $D_4$  average appears to control the upper limit of  $f_{2T}$  for the  $D_4/D_2$  ratio.

To explore the lower limit of  $f_{2T}$  for  $D_5/D_1$  and  $D_4/D_2$ , latex B was modified as summarized in Table IV. For this case, both the smallest diameter size,  $D_{21}$ , and the number of particles for the smallest particle size,  $N_{21}$ , were modified to create latexes of interest in this analysis. The results in Table IV indicate clearly that the  $D_1$  average appears to control the lower limit of  $f_{2T}$  for the  $D_5/D_1$  ratio and

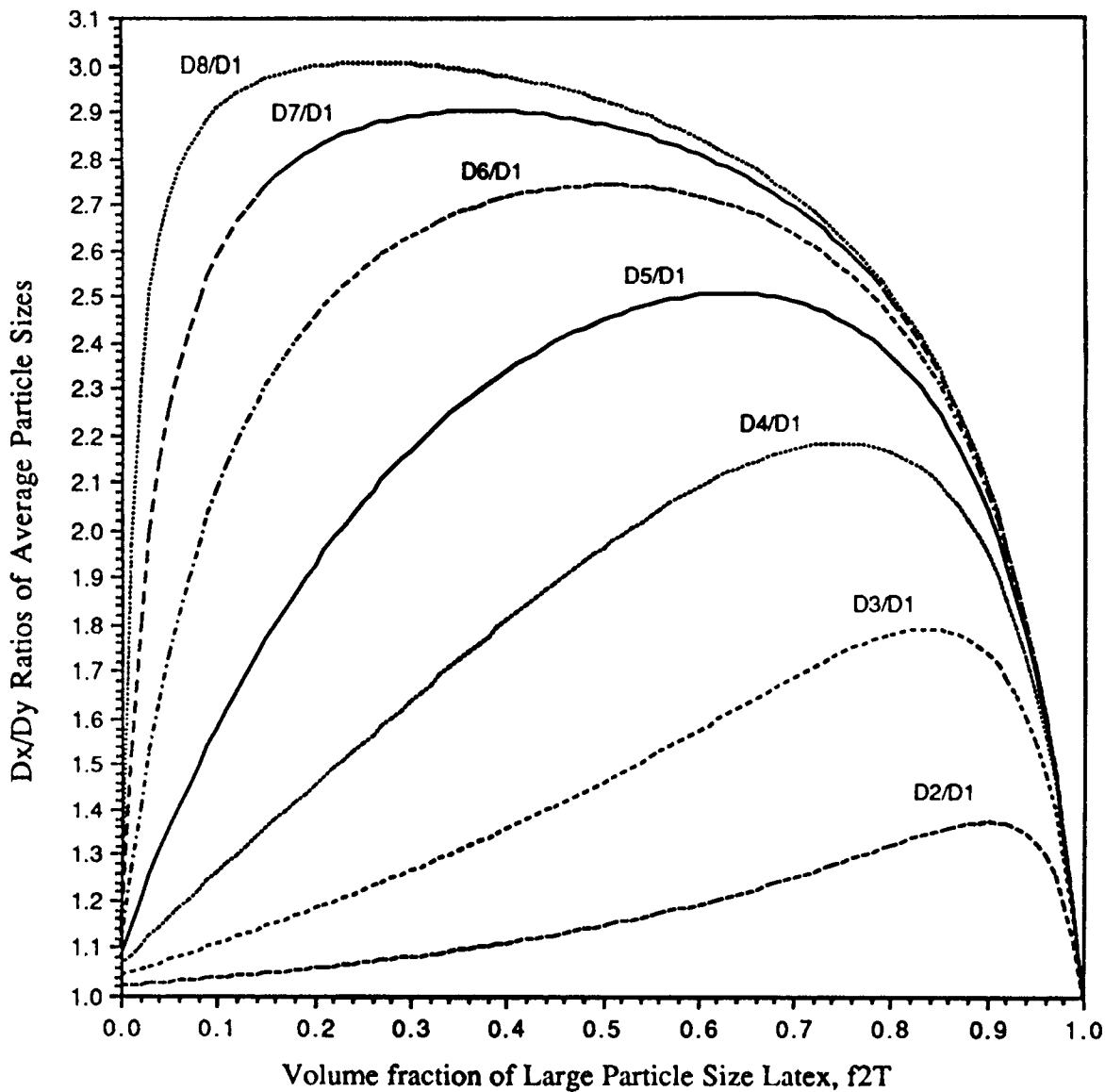


Figure 8 Theoretical blends of latexes B and D.

the  $D_2$  average appears to control the lower limit of  $f_{2T}$  for the  $D_4/D_2$  ratio.

In summary, the latex/latex blend calculations with multiple particles in both blended latexes maintain some characteristics of absolute monodisperse latex blends. However, the characteristics of interest appear to determine which  $D_x$  particle diameter average will be appropriate.

**PREDICTION OF SUSPENSION VISCOSITY PROPERTIES UTILIZING  $\phi_n$**

The influence of particle size and polydispersity on the viscosity of synthetic latexes has been studied

by Johnson and Kelsey.<sup>3</sup> By comparing loading levels of several combinations of two relatively monodisperse latexes at the same viscosity, they found that a maximum in percent solids was achieved. The effect of blending two latexes of different particle sizes to give percent solids at essentially the same 1000 cps viscosity level is shown in Figure 11. This figure illustrates that a minimum viscosity or maximum solids latex system can be obtained by suitable adjustment in both particle size and distribution.

The results shown in Figure 11 can be predicted with equations developed in this paper. This process will be illustrated using a modification of eq. (1) as given earlier in this text. This equation can be written in the form

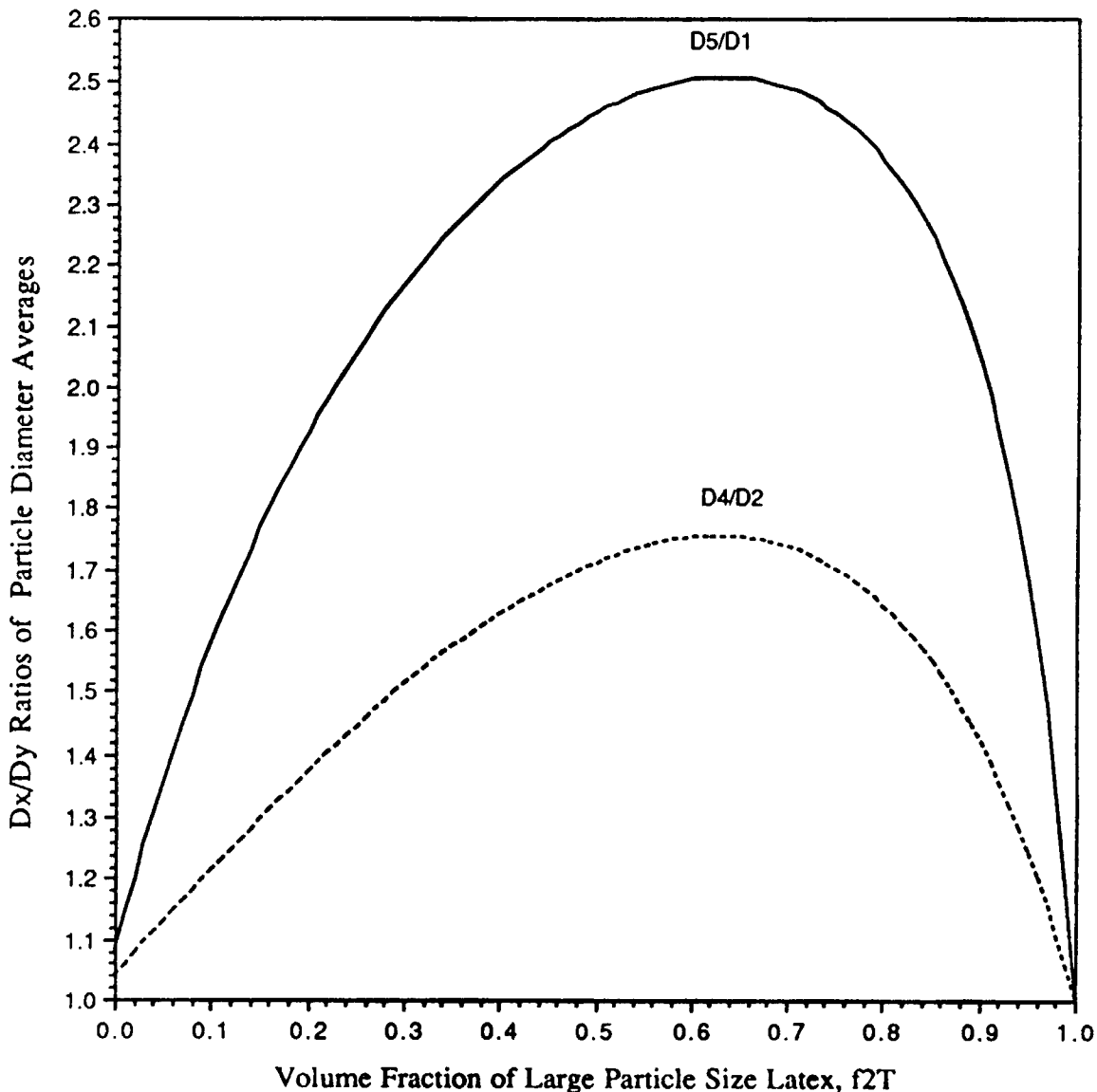


Figure 9 Calculated blends of latexes B and D.

$$\ln(\eta/\eta_0) = \left(\frac{[\eta]\varphi_n}{\sigma - 1}\right) \left\{ \left(\frac{\varphi_n - \varphi}{\varphi_n}\right)^{1-\sigma} - 1 \right\}$$

for  $\sigma \neq 1$  (35)

For the case where  $\sigma = 1$ , the resulting equation can be written as

$$\ln(\eta/\eta_0) = -[\eta]\varphi_n \ln\left(\frac{\varphi_n - \varphi}{\varphi_n}\right) \quad (36)$$

where  $\eta$  is the suspension viscosity;  $\eta_0$ , the viscosity of suspending medium;  $[\eta]$ , the intrinsic viscosity;  $\sigma$ , the particle interaction coefficient;  $\varphi$ , the suspen-

sion particle volume fraction; and  $\varphi_n$ , the maximum particle packing fraction.

In the absence of intrinsic viscosity information for the data of Kelsey and Johnson, the Einstein<sup>24</sup> limit can be assumed such that

$$[\eta] = 5/2 \quad (37)$$

The viscosity of the solution can then be determined once  $\varphi_n$  is estimated from particle-size distribution. Utilizing constants developed in an earlier paper by this author<sup>18</sup> for binary mixtures of particles, the value for  $\varphi_n$  can be obtained as

$$\varphi_n = \varphi_{nult} - (\varphi_{nult} - \varphi_m)e^{\alpha[1-(D_s/D_1)]} \quad (38)$$

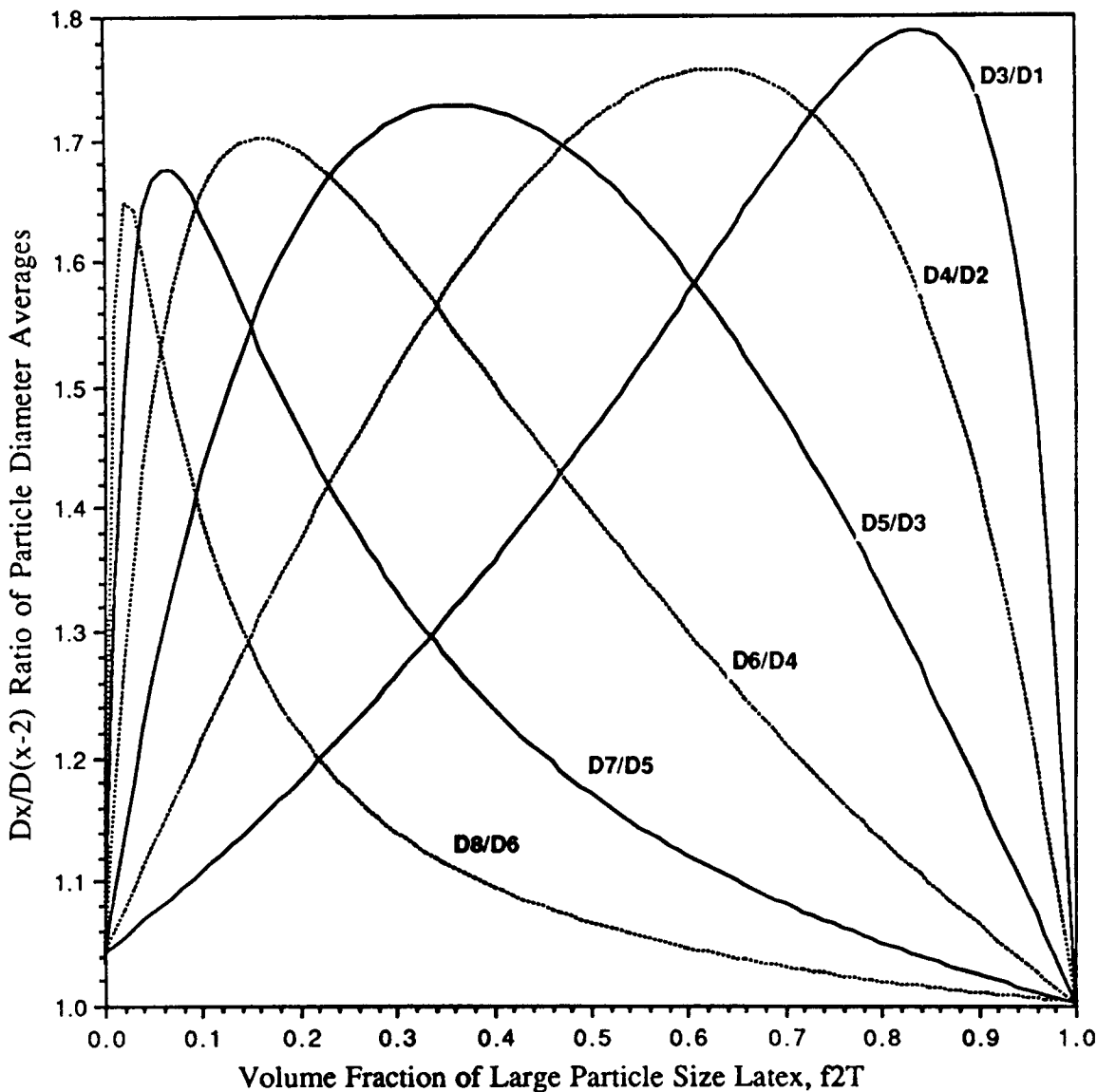


Figure 10 Blends of latex B and latex D for different average particle-size ratios,  $D_x/D_{(x-2)}$ .

$$\varphi_{\text{nult}} = 1 - (1 - \varphi_m)^n \tag{39}$$

where  $\varphi_{\text{nult}}$  is the ultimate packing fraction;  $\varphi_m$ , the monodisperse packing fraction (=0.639 from Lee<sup>21</sup>);  $\varphi_n$ , the suspension packing fraction;  $n$ , the number of different particle diameters sizes in the suspension; and  $\alpha$ , a constant (=0.268 for  $D_5/D_1$  as determined previously by this author<sup>23</sup>).

For purposes of this discussion, the density of both particles and solvents in this analysis will all be assumed to be identical to minimize calculations in converting from weight to volume. If  $f_{2T}$  is the volume fraction of the large particle size latex in a mixture of two latexes, then the  $D_5/D_1$  ratio can be

described by simplifying equations derived earlier in this paper as

$$\frac{D_5}{D_1} = \frac{A_1 f_{2T}^2 + B_1 f_{2T} + C_1}{A_2 f_{2T}^2 + B_2 f_{2T} + C_2} \tag{40}$$

where  $A_1, B_1, C_1, A_2, B_2,$  and  $C_2$  = latex blend constants [eqs. (17)] calculated using eqs. (A.8)–(A.12) and (A.22)–(A.29) in Appendix A.

If two suspensions are compared at the same viscosity but at different volume fractions,  $f_{2T}$ , they will have a constant viscosity ratio ( $\eta/\eta_0$ ). Equation (35) can then be solved for the general solution for

**Table III**  $D_x$  Particle Diameter Averages for Latexes E, EM1, EM2, and EM3

$X$	$D_x$ (Latex E)	$D_x$ (Latex EM1)	$D_x$ (Latex EM2)	$D_x$ (Latex EM3)
1	4,135.7	4,133.5	4,449.3	4,446.7
2	4,141.4	4,139.4	4,469.3	4,466.8
3	4,147.0	4,145.1	4,488.4	4,486.0
4	4,152.5	4,150.7	4,506.5	4,504.1
5	4,157.9	4,156.2	4,523.4	4,521.2
6	4,163.3	4,161.7	4,539.3	4,537.2
7	4,168.5	4,167.1	4,554.1	4,552.1
8	4,173.8	4,172.4	4,567.7	4,565.9
$D_x/D_y$	$D_5/D_1$	$D_5/D_1$	$D_4/D_2$	$D_4/D_2$
$N_{21}$	1,200	1,275	1,200	1,200
$N_{2n}$	50	50	13,500	13,250
$f_{2T}$ with latex A	0.00185616	-0.0001788	0.00032365	-0.0009893
Monodisperse diameter limit with latex A	4,158	4,158	4,506	4,506

the volume concentration,  $\varphi$ , in terms of this constant viscosity ratio ( $\eta/\eta_0$ ) as

$$\varphi = \varphi_n \left\{ 1 - \left( \frac{[\eta] \varphi_n}{(\sigma - 1) |n(\eta/\eta_0) + [\eta] \varphi_n} \right)^{1/(\sigma-1)} \right\}$$

for  $\sigma \neq 1$  (41)

When  $\sigma$  is an odd integer, a second possible solution is

$$\varphi = \varphi_n \left\{ 1 + \left( \frac{[\eta] \varphi_n}{(\sigma - 1) |n(\eta/\eta_0) + [\eta] \varphi_n} \right)^{1/(\sigma-1)} \right\}$$

for  $\sigma \neq 1$  (42)

For the case where  $\sigma = 1$ , the resulting equation can be written as

$$\varphi = \varphi_n \left\{ 1 - \left( \frac{\eta_0}{\eta} \right)^{1/([\eta] \varphi_n)} \right\} \quad (43)$$

Predicted total solids results at a viscosity of 1000 cps are shown in Figure 12 for all three binary data sets measured by Kelsey and Johnson using a constant particle interaction coefficient of  $\sigma = 1.4$ . The monodisperse packing fraction,  $\varphi_n = 0.639$ , used in this calculation was originally obtained by Lee<sup>21</sup> from an average of five literature values for dense random monodisperse packing. The constant vis-

**Table IV**  $D_x$  Particle Diameter Averages for Latexes BM1, BM2, BM3, and BM4

$X$	$D_x$ (Latex BM1)	$D_x$ (Latex BM2)	$D_x$ (Latex BM3)	$D_x$ (Latex BM4)
1	654.1	656.7	978.0	979.9
2	808.2	810.8	1,007.8	1,009.2
3	940.9	942.6	1,036.2	1,037.3
4	1,027.3	1,028.1	1,063.0	1,063.8
5	1,078.3	1,078.7	1,088.1	1,088.6
6	1,110.8	1,111.0	1,111.4	1,111.8
7	1,134.9	1,134.9	1,133.0	1,133.2
8	1,155.0	1,155.0	1,153.0	1,153.1
$D_x/D_y$	$D_5/D_1$	$D_5/D_1$	$D_4/D_2$	$D_4/D_2$
$N_{21}$	14,250	14,000	1,400	1,325
$D_{21}$	400	400	700	700
$f_{2T}$ with latex A	0.00046812	-0.0103013	0.00127045	-0.0005149
Monodisperse diameter limit with latex A	673	673	1,009	1,009



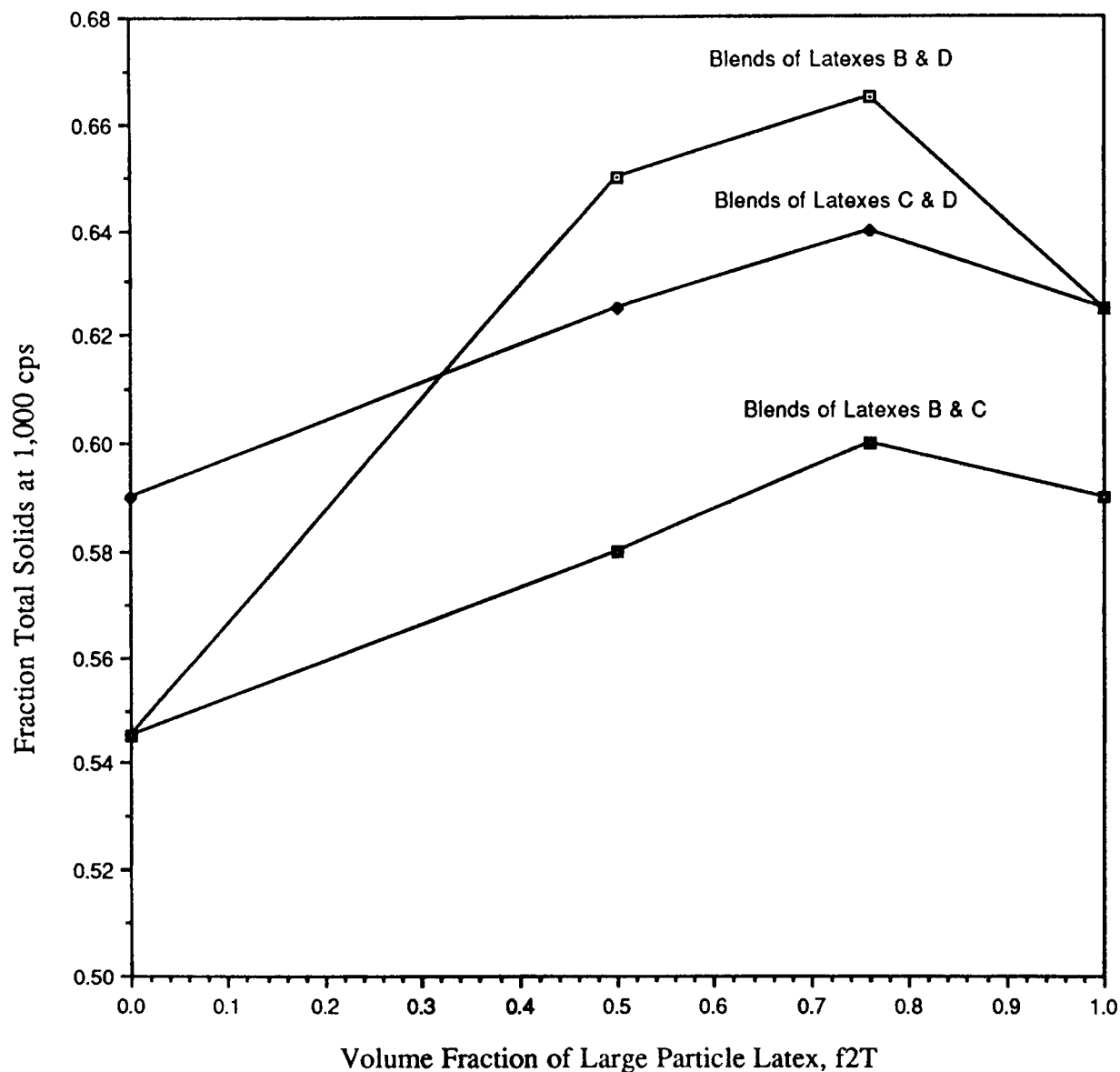


**Figure 11** Viscosity data of Johnson and Kelsey at 1000 cps for blends of latexes B, C, and D.

cosity ratio,  $\eta/\eta_0$ , was calculated from the viscosity blend data for each of the three binary latex blend combinations at a large particle latex volume fraction of  $f_{2T} = 0.76$ . The general ranges and shapes of the curves for these calculated results were very similar to the measured results of Kelsey and Johnson. More importantly, when the particle interaction coefficient,  $\sigma$ , is a constant, the solids fractions,  $\phi$ , is a direct function of only the packing fraction,  $\phi_n$ . For this case, it can easily be shown that the maximum value for  $\phi$  obtained by setting the derivative of eq. (41) equal to zero will yield the same location of the maximum relative to the composition volume

fraction,  $f_{2T}$ , as the packing fraction,  $\phi_n$ . However, at  $f_{2T} = 0$  and at  $f_{2T} = 1.0$ , the solids fractions,  $\phi$ , are nearly identical with only a slight difference between these end points indicative of the initial distribution of these separate latexes. Unfortunately, the effects of distribution at these end points was opposite to that indicated by the data.

The unexpected difference in the viscosity at these end points was postulated by Kelsey and Johnson to be related to the contribution of the smaller-size particles. If the small particles are indeed making a major contribution to the viscosity, then it would be expected that the particle inter-

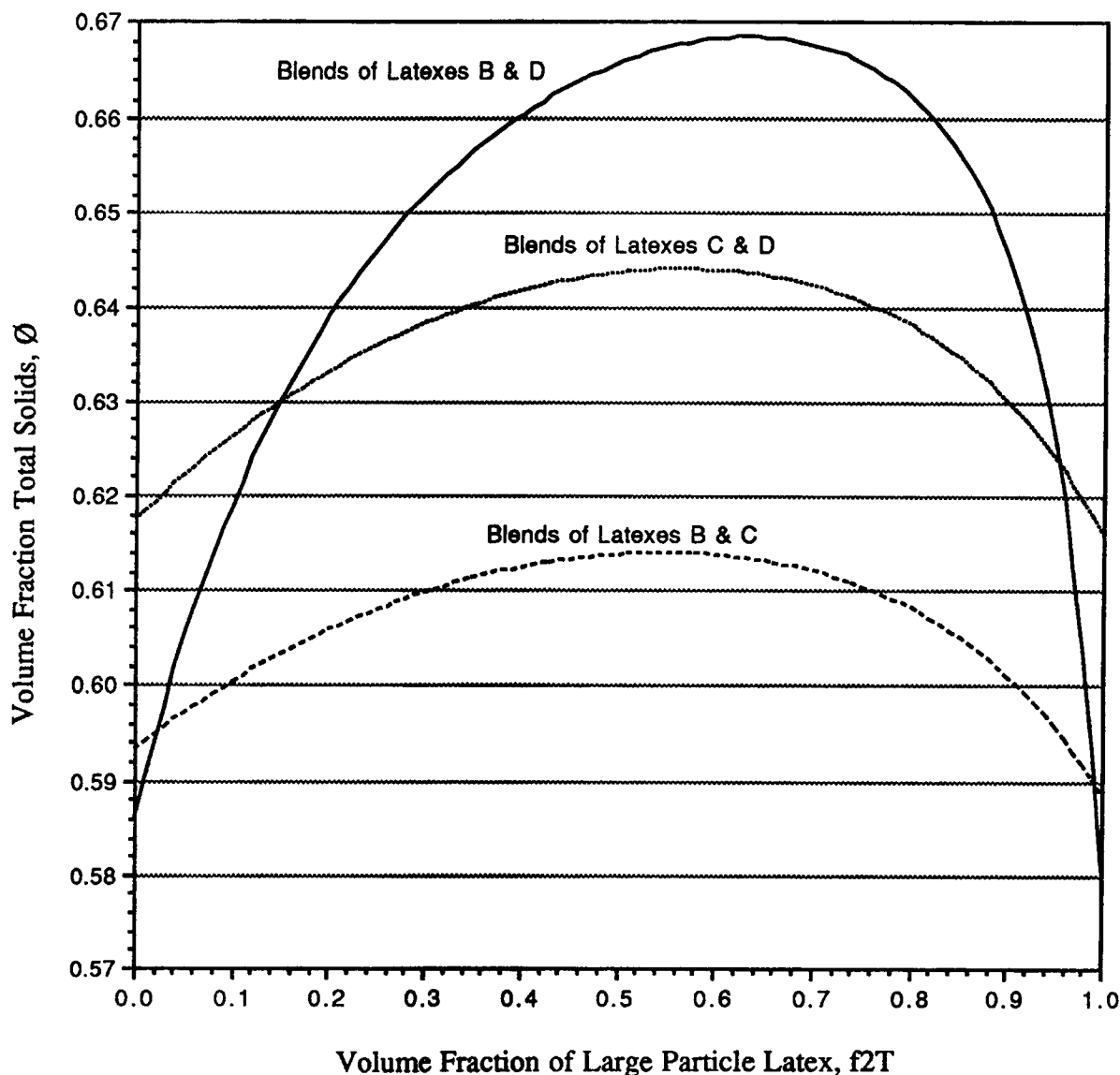


Figure 12 Calculated volume fraction solids for a constant particle interaction coefficient.

action coefficient would change with the quantity of small particles.

In a previous article by this author,<sup>17</sup> the particle interaction coefficient was shown to be theoretically separable into a contribution predominantly from the interaction of particles with each other and another part associated with the interaction of particles with solvent. One formulation discussed for the particle-particle interaction involved the number-average particle diameter,  $D_1$ , yielding a particle interaction coefficient,  $\sigma$ , function of the form

$$\sigma = \frac{\sigma_{PC}}{D_1} + \sigma_S \quad (44)$$

where  $\sigma_{PC}$  is a constant associated with the particle-particle contribution to the particle interaction coefficient and  $\sigma_S$  is a constant associated with the particle-solvent contribution to the particle interaction coefficient and where  $D_1$  can be obtained as a function of  $f_{2T}$  [from a modification of the earlier eq. (15)] as

$$D_1 = \mathcal{D}_{11} \left\{ \frac{d_1 + f_{2T}(d_2 - d_1)}{b_1 + f_{2T}(b_2 - b_1)} \right\} \quad (45)$$

where  $\mathcal{D}_{11}$  is the diameter of the first particle in the first suspension and  $b_1, b_2, d_1$ , and  $d_2$  are latex blend

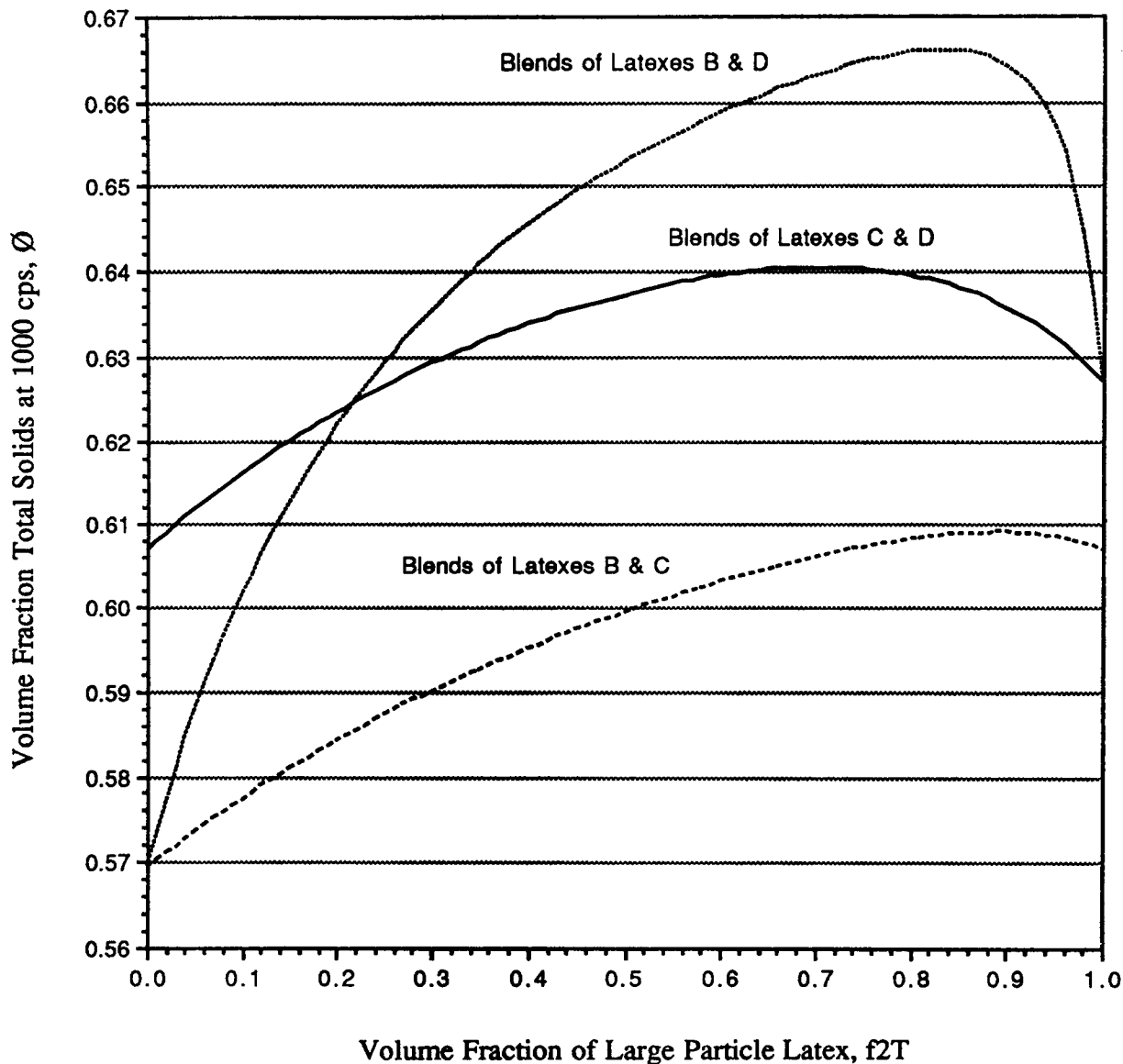


**Figure 13** Calculated volume fraction total solids for a variable particle interaction coefficient.

constants calculated using eq. (A.24), (A.25), (A.28), and (A.29) in Appendix A.

When  $\sigma$  is allowed to vary with the number-average particle diameter,  $D_1$ , as indicated in eqs. (44) and (45), then a significant improvement in the calculated fit of the measured data results as indicated in Figure 13. The constant viscosity ratio,  $\eta/\eta_0$ , used for all three binary latex blend combinations was calculated at a volume fraction of large particles of  $f_{2T} = 0.76$  using only the viscosity data involving latexes B and D. With  $D_1$  calculated in angstroms as reported by Kelsey and Johnson, the best data fit of eq. (44) gave

$$\sigma = \frac{773.6}{D_1} + 0.750 \quad (46)$$

These same constants for  $\sigma$  were also used to fit the blends for latexes B and C as well as the blends for latexes C and D. In addition, the constant viscosity ratio,  $\eta/\eta_0$ , was also used for the C/D and B/C latex blends. The actual values for  $\sigma$  calculated using eq. (46) are given in Figure 14 as a function of  $f_{2T}$ . Note that the values of  $\sigma$  for these three sets of latexes varied from 0.994 to 1.513. It is particularly interesting to note that the value of the particle interaction coefficient,  $\sigma$ , increased with a decrease in

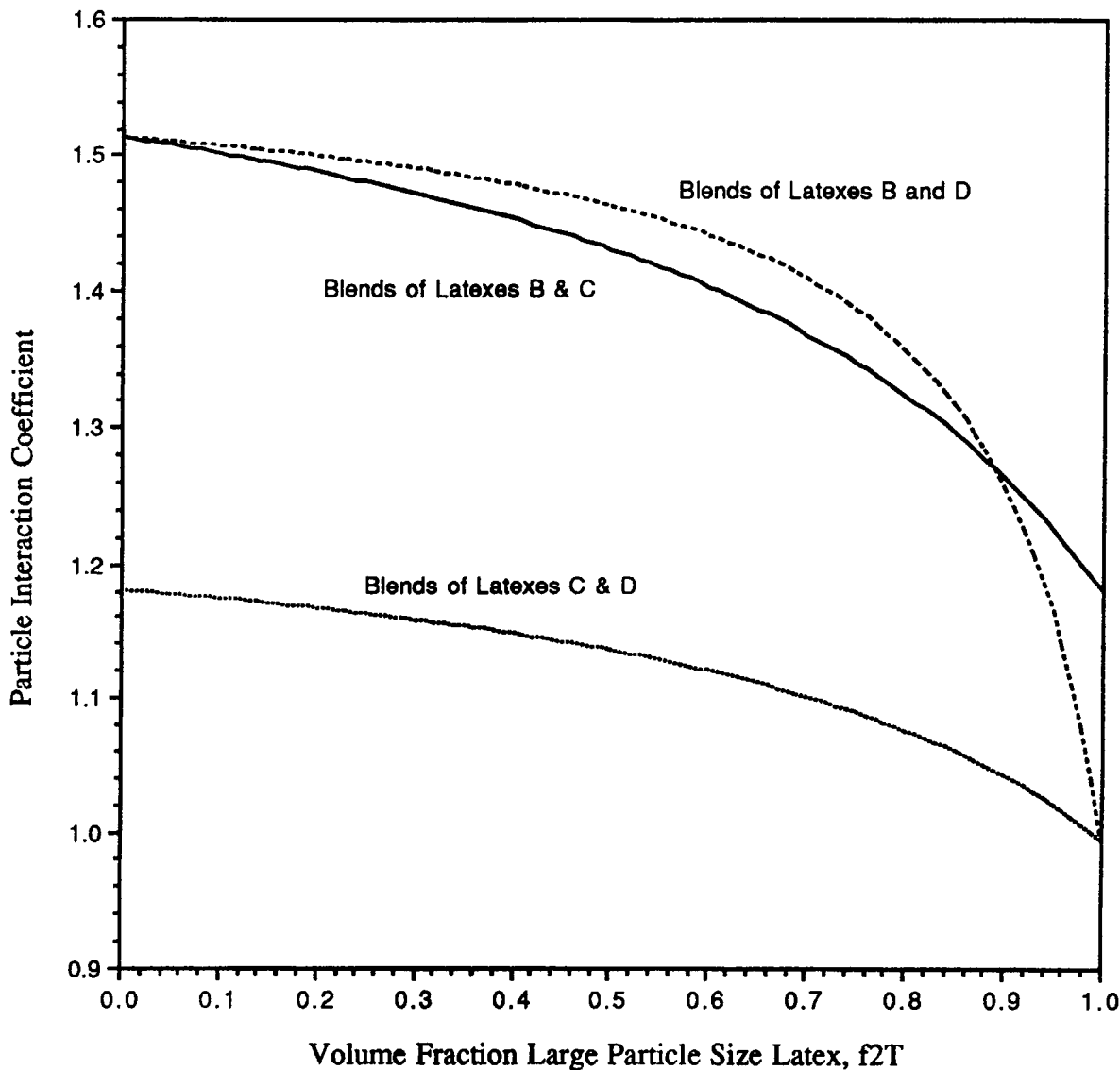


Figure 14 Variable particle interaction coefficient vs. volume fraction,  $f_{2T}$ .

the number-average particle size,  $D_1$ , and, consequently, an increase in the number of smaller particles. Such an increase in the particle interaction coefficient would be expected to result in an increase in viscosity. However, at the same time, some increase in the number of small particles did improve the viscosity by increasing the particle-size distribution as measured by the  $D_5/D_1$  ratio.

In this study, a clear separation has been made of the effects of small particles to both improve viscosity by improving the particle-size distribution, but at the same time to decrease viscosity performance due to increased particle interaction. However, it is equally apparent that additional data is needed to confirm this conclusion.

The location of the minimum viscosity or maximum solids fraction at constant viscosity is somewhat different for the blend of latexes B and D as indicated in Figure 15 depending on whether  $\sigma$  is held constant or is allowed to vary. The specific results show that the location of the maxima for these two cases are

$$f_{2T} = 0.63 \text{ (when } \sigma \text{ is a constant)} \quad (47)$$

and

$$f_{2T} = 0.83 \text{ (when } \sigma \text{ is allowed to be a variable)} \quad (48)$$

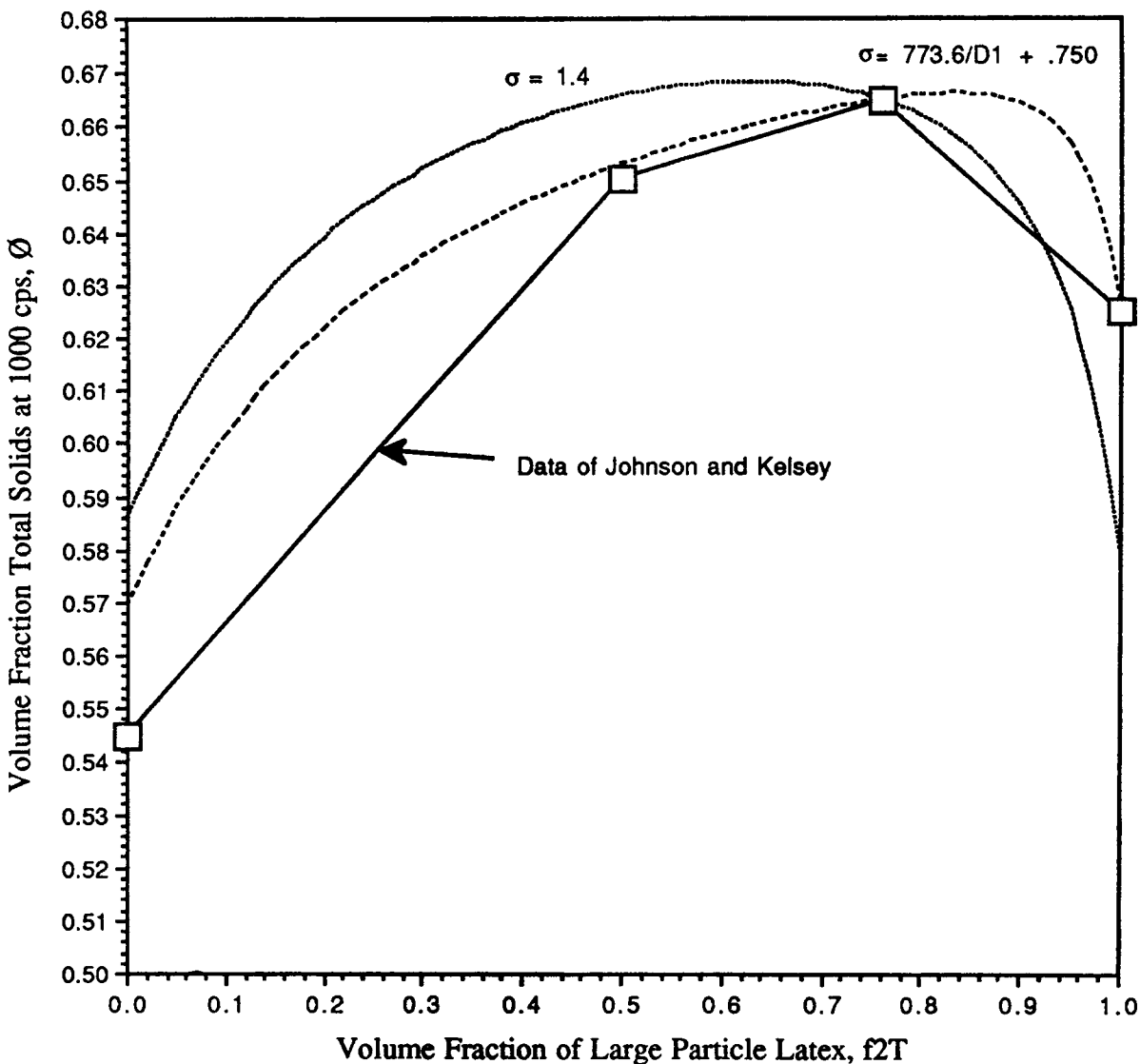


Figure 15 Data of Johnson and Kelsey compared with theoretical total solids at a viscosity of 1000 cps for both constant and variable particle interaction coefficient.

Although the location of the maxima is different for these two cases, it is interesting that the maximum fraction solids,  $\phi$ , for these two cases was nearly identical. However, when both of these two predicted viscosity curves are compared with the actual data of Johnson and Kelsey in Figure 15, it appears that a variable particle interaction coefficient gives the best fit of the data.

Finally, while results in Figure 15 show only the data results at a viscosity of 1000 cps, the results in Figure 16 show the complete viscosity curves for the B/D latex combinations developed by Johnson and Kelsey. Note specifically that the subtle shifts in these blended latex viscosity curves can be predicted

very satisfactorily using only calculations obtained from particle-size distribution. Although the viscosity curve for latex B by itself was not predicted very satisfactorily, it is apparent that curves for the blends were predicted very well. More importantly, note that the improved properties of the latex blends compared to the viscosity curves of the two original latexes were predicted very satisfactorily.

## CONCLUDING REMARKS

The generalized suspension viscosity equation utilized in this study was evaluated with both a packing

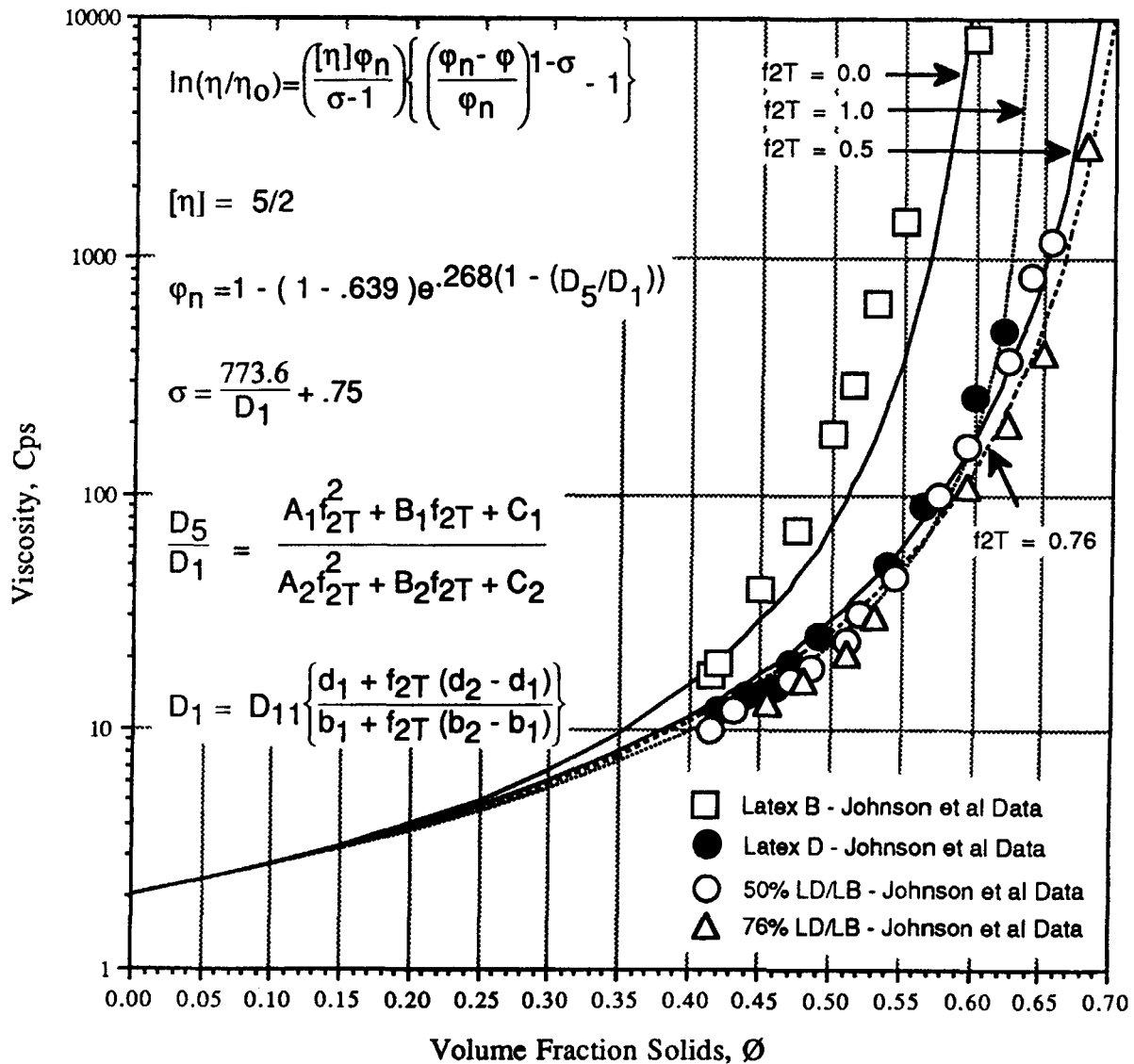


**Figure 16** Viscosity data of Johnson and Kelsey compared with theoretical predictions for the blends of latexes B and D.

fraction,  $\phi_n$ , and a particle interaction coefficient,  $\sigma$ , as a function of suspension blend composition,  $f_{2T}$ . The estimation of the packing fraction,  $\phi_n$ , in turn, required the further elucidation of the  $D_5/D_1$  ratio of particle diameter averages. Blend constants developed in this study allowed evaluation of both the  $D_x/D_y$  ratio of particle diameter averages as well as the number-average particle diameter,  $D_1$ , as a function of the fraction of one suspension in a blend,  $f_{2T}$ . These blend constants were shown to be easily evaluated from each individual suspension prior to blending.

The calculated variations of  $D_x/D_y$  ratios were evaluated by mathematically blending monodisperse

suspensions as well as by adding several monodisperse suspensions to a broad particle-size suspension. In general, results found previously for absolute monodisperse blends were found not to apply exactly to blends of moderately distributed monodisperse suspensions. It was also found that there was a diameter range of exact monodisperse latexes that could not improve the maximum  $D_5/D_1$  distribution ratio of the broad particle-size suspension independent of the amount of monodisperse latex added.

The viscosity data of Johnson and Kelsey<sup>3</sup> were shown to be generally predicted as a function of the volume composition when a constant particle interaction coefficient,  $\sigma$ , was assumed. However, a better

prediction of the results of Johnson and Kelsey was obtained by assuming that the particle interaction coefficient,  $\sigma$ , was a function the number-average particle diameter,  $D_1$ , of the suspension mixture composition. The effectiveness of the number average in predicting  $\sigma$  appears to be related to the contribution that the small particles play in determining the contribution to the suspension viscosity. It was found that as the number of small particles increased that the value of the particle interaction coefficient,  $\sigma$ , increased. Such an increase in the particle interaction coefficient would result in an increase in viscosity. However, at the same time, some decrease in viscosity resulted from an increase in the broadness of the particle-size distribution due to the small particle-size contribution as measured by the  $D_5/D_1$  ratio. Consequently, this study identified a new approach to separate effects of small particles to both improve viscosity by improving the particle-size distribution but at the same time to decrease viscosity performance due to increased particle interaction.

Unfortunately, the data of Johnson and Kelsey appears to be insufficient to establish a clear understanding of the optimized balance between particle interaction and particle-size distribution. Future work and additional data are needed.

Nevertheless, the results from this study show how viscosity results can be predicted directly from an evaluation of particle-size distribution. In particular, it has been shown that particle-size distribution can potentially be used to predict the composition that will give the lowest viscosity or the maximum fraction solids for blends of suspensions.

## APPENDIX A: DERIVATION OF SELECTED BLEND CONSTANTS FOR A BLEND OF TWO LATEXES

For a mixture of two suspensions then the ratio of a  $D_x$  average diameter to the  $D_y$  average diameter can be written as

$$\frac{D_x}{D_y} = \left\{ \frac{\sum_{i=1}^n N_{1i} \mathcal{D}_{1i}^x + \sum_{j=1}^m N_{2j} \mathcal{D}_{2j}^x}{\sum_{i=1}^n N_{1i} \mathcal{D}_{1i}^{x-1} + \sum_{j=1}^m N_{2j} \mathcal{D}_{2j}^{x-1}} \right\} \times \left\{ \frac{\sum_{i=1}^n N_{1i} \mathcal{D}_{1i}^{y-1} + \sum_{j=1}^m N_{2j} \mathcal{D}_{2j}^{y-1}}{\sum_{i=1}^n N_{1i} \mathcal{D}_{1i}^y + \sum_{j=1}^m N_{2j} \mathcal{D}_{2j}^y} \right\} \quad (\text{A.1})$$

The process of simplifying eq. (A.1) begins by considering the volume fraction of different particles prior to

blending. For example, the volume fraction of the first particle,  $f_{11}$ , in the first suspension before blending can be described as

$$f_{11B} = \frac{N_{11B} \mathcal{D}_{11}^3}{\sum_{i=1}^n N_{1iB} \mathcal{D}_{1i}^3} \quad (\text{A.2})$$

Similarly, the volume fraction of the first particle,  $f_{21}$ , in the second suspension before blending can be described as

$$f_{21B} = \frac{N_{21B} \mathcal{D}_{21}^3}{\sum_{j=1}^m N_{2jB} \mathcal{D}_{2j}^3} \quad (\text{A.3})$$

However, after the two suspensions are blended, then the volume fraction of the first particle in the blend would be defined as

$$f_{11} = \frac{N_{11} \mathcal{D}_{11}^3}{\sum_{i=1}^n N_{1i} \mathcal{D}_{1i}^3 + \sum_{j=1}^m N_{2j} \mathcal{D}_{2j}^3} \quad (\text{A.4})$$

Using volume fractions as described by eq. (A.4), the sum of all particle fractions in the blend would equal 1 as

$$f_{11} + f_{12} + f_{13} + \cdots + f_{1n} + f_{21} + f_{22} + f_{23} + \cdots + f_{2m} = 1 \quad (\text{A.5})$$

However, eq. (A.5) can be rewritten as

$$f_{11} (1 + K_{12} + K_{13} + \cdots + K_{1n}) + f_{21} (1 + K_{22} + K_{23} + \cdots + K_{2m}) = 1 \quad (\text{A.6})$$

or

$$f_{11} \left( \sum_{i=1}^n K_{1i} \right) + f_{21} \left( \sum_{j=1}^m K_{2j} \right) = 1 \quad (\text{A.7})$$

where

$$K_{1i} = \frac{f_{1i}}{f_{11}} = \frac{N_{1i} \mathcal{D}_{1i}^3}{N_{11} \mathcal{D}_{11}^3} \quad (\text{A.8})$$

and

$$K_{2j} = \frac{f_{2j}}{f_{21}} = \frac{N_{2j} \mathcal{D}_{2j}^3}{N_{21} \mathcal{D}_{21}^3} \quad (\text{A.9})$$

Note that all values of  $K_{1i}$  and  $K_{2j}$  and their separate sums in eqs. (A.6) and (A.7) are constants and independent of composition. This is true since all values of  $N_{1i}$  and all values of  $N_{2j}$  will always change in the same proportion when one suspension is added to another. How-

ever, to simplify eqs. (A.8) and (A.9) even further, it is important to define the following binary ratios within each suspension as

$$R_{1i} = \frac{D_{1i}}{D_{11}} \quad (\text{A.10})$$

and

$$R_{2j} = \frac{D_{2j}}{D_{21}} \quad (\text{A.11})$$

One additional specific binary ratio,  $R_{21/11}$ , also needs to be defined as

$$R_{21/11} = \frac{D_{21}}{D_{11}} \quad (\text{A.12})$$

Combining eqs. (A.8) and (A.10) gives

$$\frac{N_{1i}}{N_{11}} = K_{1i} R_{1i}^{-3} \quad (\text{A.13})$$

Combining eqs. (A.9) and (A.11) gives

$$\frac{N_{2j}}{N_{21}} = K_{2j} R_{2j}^{-3} \quad (\text{A.14})$$

An additional important ratio that relates both blended suspensions to each other can be defined as

$$\frac{f_{21}}{f_{11}} = \frac{N_{21} D_{21}^3}{N_{11} D_{11}^3} \quad (\text{A.15})$$

Combining eqs. (A.7), (A.12), and (A.15) gives

$$\frac{N_{21}}{N_{11}} = \left\{ \frac{f_{21} \sum_{i=1}^n K_{1i}}{1 - f_{21} \sum_{j=1}^m K_{2j}} \right\} R_{21/11}^{-3} \quad (\text{A.16})$$

Equation (A.16) can be further simplified if it is noted that the total volume fraction of all particles in suspensions 1 and 2 can be combined into single total fractions,  $f_{1T}$  and  $f_{2T}$ , which can be calculated as

$$f_{1T} = f_{11} \sum_{i=1}^n K_{1i} \quad (\text{A.17})$$

$$f_{2T} = f_{21} \sum_{j=1}^m K_{2j} \quad (\text{A.18})$$

such that for any combination of suspensions eq. (A.7) simplifies to

$$f_{1T} + f_{2T} = 1 \quad (\text{A.19})$$

Substituting eqs. (A.18) and (A.19) into eq. (A.16) gives

$$\frac{N_{21}}{N_{11}} = \left\{ \frac{f_{2T} \left( \frac{\sum_{i=1}^n K_{1i}}{\sum_{j=1}^m K_{2j}} \right)}{1 - f_{2T}} \right\} R_{21/11}^{-3} \quad (\text{A.20})$$

At this point, utilizing eqs. (A.10)–(A.14) and (A.20) allow the  $D_x/D_y$  ratio in eq. (A.1) to be simplified as

$$\frac{D_x}{D_y} = \left\{ \frac{a_1 + f_{2T}(a_2 - a_1)}{c_1 + f_{2T}(c_2 - c_1)} \right\} \left\{ \frac{b_1 + f_{2T}(b_2 - b_1)}{d_1 + f_{2T}(d_2 - d_1)} \right\} \quad (\text{A.21})$$

where

$$a_1 = \sum_{i=1}^n K_{1i} R_{1i}^{x-3} \quad (\text{A.22})$$

$$a_2 = \left( \frac{\sum_{i=1}^n K_{1i}}{\sum_{j=1}^m K_{2j}} \right) R_{21/11}^{x-3} \sum_{j=1}^m K_{2j} R_{2j}^{x-3} \quad (\text{A.23})$$

$$b_1 = \sum_{i=1}^n K_{1i} R_{1i}^{y-4} \quad (\text{A.24})$$

$$b_2 = \left( \frac{\sum_{i=1}^n K_{1i}}{\sum_{j=1}^m K_{2j}} \right) R_{21/11}^{y-4} \sum_{j=1}^m K_{2j} R_{2j}^{y-4} \quad (\text{A.25})$$

$$c_1 = \sum_{i=1}^n K_{1i} R_{1i}^{x-4} \quad (\text{A.26})$$

$$c_2 = \left( \frac{\sum_{i=1}^n K_{1i}}{\sum_{j=1}^m K_{2j}} \right) R_{21/11}^{x-4} \sum_{j=1}^m K_{2j} R_{2j}^{x-4} \quad (\text{A.27})$$

$$d_1 = \sum_{i=1}^n K_{1i} R_{1i}^{y-3} \quad (\text{A.28})$$

$$d_2 = \left( \frac{\sum_{i=1}^n K_{1i}}{\sum_{j=1}^m K_{2j}} \right) R_{21/11}^{y-3} \sum_{j=1}^m K_{2j} R_{2j}^{y-3} \quad (\text{A.29})$$

## REFERENCES

1. M. Mooney, *J. Colloid Sci.*, **6**(2), 162–170 (1951).
2. S. H. Maron and B. P. Madow, *J. Colloid Sci.*, **8**, 130–136 (1953).
3. P. H. Johnson and R. H. Kelsey, *Rubber World*, **138**, 877–882 (1958).



4. I. M. Krieger and T. J. Dougherty, *Trans. Soc. Rheol.*, **3**, 137-152 (1959).
5. K. L. Hoy, in *Organic Coatings Science and Technology*, G. D. Parfitt and A. V. Patis, Eds., Marcel Dekker, New York, 1983, Vol. 5.
6. R. Van Gilder, D. I. Lee, R. Purfeerst, and J. Allswede, *TAPPI J.*, **66**(11), 49-53 (1983).
7. A. Leviton and A. Leighton, *J. Phys. Chem.*, **40**(71), 51-59 (1936).
8. H. Eilers, *Koll. Z.*, **97**, 913 (1941).
9. J. A. De Sousa, in *Advances in Rheology, Vol. 3: Polymers, Proceedings IX International Congress of Rheology, Mexico*, B. Mena, A. Garcia-Rejon, and C. Rangel-Nafaile, Eds., Universidad Nacional Autonoma De Mexico, Mexico, 1984, pp. 439-446.
10. D. M. Bigg, in *Advances in Rheology, Vol. 3: Polymers, Proceedings IX International Congress of Rheology, Mexico*, B. Mena, A. Garcia-Rejon, and C. Rangel-Nafaile, Universidad Nacional Autonoma De Mexico, Mexico, 1984, pp. 429-437.
11. A. I. Leonov, *J. Rheol.*, **34**(7), 1039-1068 (1990).
12. H. G. Recker, T. Allspach, V. Altstadt, T. Folda, W. Heckmann, P. Itteman, H. Tessch, and T. Weber, *SAMPE Q.*, **October**, 46-51 (1989).
13. H. A. Barnes, *J. Rheol.*, **33**(2), 329-366 (1989).
14. H. A. Barnes, J. F. Hutton, and K. Walters, *An Introduction to Rheology*, Elsevier, Amsterdam, 1989, pp. 119-125.
15. A. B. Metzner, *J. Rheol.*, **29**, 739 (1985).
16. C. Tsenoglou, *J. Rheol.*, **34**(1), 15-24 (1990).
17. R. D. Sudduth, *J. Appl. Polym. Sci.*, **48**, 25 (1993).
18. I. R. Rutgers, *Rheol. Acta*, **2**, 202 (1962).
19. I. R. Rutgers, *Rheol. Acta*, **2**, 305 (1962).
20. R. K. McGeary, *J. Am. Ceram. Soc.*, **44**(10), 513-522 (1961).
21. D. I. Lee, *Paint Technol.*, **42**(550), 579-587 (1970).
22. K. L. Hoy, in *Organic Coatings Science and Technology*, G. D. Parfitt and A. V. Patis, Eds., Marcel Dekker, New York, 1983, Vol. 5, pp. 123-146.
23. R. D. Sudduth, *J. Appl. Polym. Sci.*, **48**, 37 (1993).
24. A. Einstein, *Ann. Phys.*, **19**, 289-306 (1906).
25. A. Einstein, *Ann. Phys.*, **34**, 591-592 (1911).
26. Arrhenius, *Z. Physik. Chem.*, **1**, 285 (1887).
27. Arrhenius, *Biochem. J.*, **11**, 112 (1917).
28. G. Herdan, *Small Particle Statistics*, Elsevier, New York, 1953, pp. 46-60.
29. R. D. Sudduth, *J. Appl. Polym. Sci.*, **22**, 2427-2334 (1978).

Received March 4, 1992

Accepted January 14, 1993